$NADP^+$-dependent isocitrate dehydrogenase activity in the marine plankton community

Mayte Tames-Espinosa, Ico Martínez, Vanesa Romero-Kutzner, Daniel Rickue Bondyale-Juez, Theodore T. Packard and May Gómez[a]

[a]*Marine Ecophysiology Group (EOMAR), IU-ECOAQUA, Universidad de Las Palmas de Gran Canaria, Campus Universitario de Tafira 35017, Las Palmas de Gran Canaria, Canary Islands, Spain*

Abstract

$NADP^+$-isocitrate dehydrogenase (NADP-IDH), as one of the most active intracellular CO_2-producing enzymes, was measured in the marine plankton community by adapting an enzyme assay to the 0.7-50μm, 50-200μm, and 200-2000μm size fraction of the Canary Islands coastal plankton community. The variability of NADP-IDH activity in relation to pH, T, dilution of the sample, centrifugation or substrates was measured. In our hands, the maximum NADP-IDH activity (V_{max}) in marine plankton samples was attained in 0.1M phosphate buffer at pH 8.2 (pKa_1=7.6 and pKa_2=8.8), by adding 6mM $MgCl_2$, 0.3mM $NADP^+$ and 2mM DL-trisodium isocitrate. The optimum temperature in these subtropic mesozooplankton samples was 28°C, with an Arrhenius energy of activation (Ea) of 20.4 Kcal mol^{-1} (85.4J mol^{-1}), and an Arrhenius collision frecuency factor (A) of $2.9{\cdot}10^{11}$ mol NADPH s^{-1} (Kg of protein)$^{-1}$. The apparent Michaelis-Menten Km values for the substrates in crude homogenates at pH 8.5 and 18°C were 232±34 μM for isocitrate and 22±7 μM for $NADP^+$. This enzyme, in addition to its high CO_2-producing activity, is also important in regulating other CO_2-producing enzymes. Thus, it can be used to calculate: (1) respiration in marine samples; (2) carbon flux in the water column; (3) metabolic adaptations to environmental changes; (4) roles of the plankton components of the food chain; and (5) the reactive oxygen species (ROS) scavenging capacity of the marine plankton resources.

Keywords: Carbon flux, $NADP^+$-dependent isocitrate dehydrogenase, Plankton metabolism, Cellular respiration, Metabolic measurements, Marine ecology

1. Introduction

Since the 1980s, the assessment and understanding of the processes that control the carbon fluxes between atmosphere, the marine surface waters, the deep ocean, and the benthos, have been the focus of international research programs (e.g., Joint Global Ocean Flux Study, JGOFS). One of the processes that impact on the carbon fluxes in the ocean is the CO_2 production related to respiration. However, in oceanography, there are constraints in determining CO_2 changes in seawater (Mayzaud et al. [21]), so respiratory rates have mainly been reported as O_2 consumption. As a result, respiratory quotients (RQs), ratios between CO_2 produced and O_2 consumed, are required to calculate respiratory CO_2 production rates from either direct O_2 consumption measurements (Berggren et al. [6], Romero-Kutzner et al. [38]), from calculations of O_2 consumption from ETS activity measurements (Hernández-Leon et al. [13], Osma et al. [29, 30], Packard and Codispoti [33], Packard and Gómez [34]), or from biomass (Steinberg et al. [46]). The fact that RQ is now known to be more variable than expected (Berggren et al. [6], Romero-Kutzner et al. [38]) adds impetus to developing methodology to assess seawater CO_2 production rates more directly.

Here, we propose to assess this process enzymatically. The biochemistry of respiratory CO_2 production is dominated by $NAD(P)^+$- dependent isocitrate dehydrogenase in the Krebs cycle (IDH_{KC} in Fig. 1) (Nelson and Cox [26]). In cells, other biochemical reactions produce CO_2, but their production rates can be predicted from IDH_{KC} activity (Packard et al. [32], Roy and Packard [39], Tames-Espinosa et al. [48]). Of those linked to respiration, pyruvate dehydrogenase (PDH in Fig.1) serves to bridge the metabolism of glucose (glycolysis) to the Krebs cycle. Then, inside this cycle of enzyme reactions, both IDH_{KC} and alpha-ketoglutarate dehydrogenase (KGDH in Fig. 1), produce CO_2, being the IDH_{KC} activity 1.1 times the KGDH activity (Walsh and Koshland [49], Fig.1). Finally, linked to, but not in the Krebs cycle, are the malic enzyme (ME in Fig. 1) and phosphoenol pyruvate carboxykinase (PEPCK in Fig. 1). They also generate CO_2 but at much reduced rates. IDH_{KC} activity is 8.4 times greater than these activities.

IDH_{KC} encompass two isoenzymes that catalyse the conversion of isocitrate to α - ketoglutarate in a reaction summarized in Equation 1 (Nelson and Cox [26]).

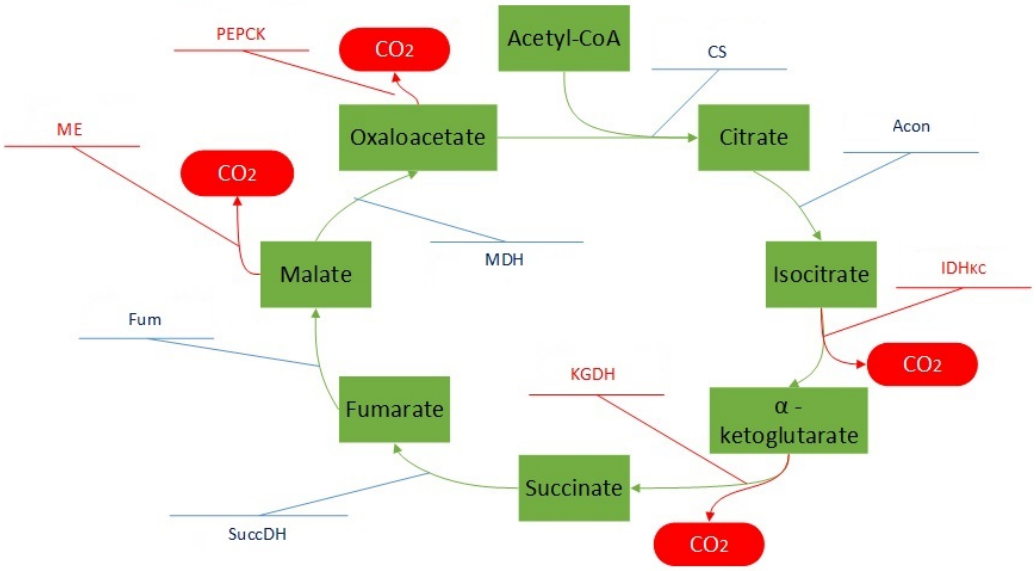

Figure 1: Main Krebs cycle reactions in the bacterium, *Escherichia coli*, during acetate utilisation, redrawn from Walsh and Koshland [49] (1984). Abbreviations and CO_2-producing enzymes activity rates are: CS, citrate synthase; Acon, aconitase; IDH_{KC}, isocitrate dehydrogenase (80mmol of substrate consumed min^{-1} L^{-1} of cell volume) linked to the Krebs cycle; KGDH, α-ketoglutarate dehydrogrenase (75mmol of substrate consumed min^{-1} L^{-1} of cell volume); SuccDH, succinate dehydrogenase; Fum, fumarase; MDH, malate dehydrogenase; ME, malic enzyme (9.5mmol of substrate consumed min^{-1} L^{-1} of cell volume); PEPCK, phosphoenolpyruvate carboxykinase (9.5mmol of substrate consumed min^{-1} L^{-1} of cell volume). Note that reactions linked to CO_2 production have been highlighted in red.

$$\text{Isocitric acid} + \text{NAD(P)}^+ \leftrightarrow \alpha\text{ -ketoglutaric acid} + NAD(P)H + CO_2 (1)$$

where 1 mol of CO_2 is stoichiometrically related to the production of 1 mol of NAD(P)H.

These enzymes can be either NAD^+ or $NADP^+$-dependent (NAD-IDH or NADP-IDH respectively) (Kornberg and Pricer [18], Gálvez and Gadal [11]). However, unlike NAD-IDH, NADP-IDH is ubiquitous in all kind of organisms (from *E.coli*-liked bacteria to plants and mammals); its activity has been reported to be up to 10-fold greater than NAD-IDH activity (Alp et al. [2], Colman [7], Denton et al. [9]); and, unlike NAD-IDH, NADP-IDH is stable during the measurement (Plaut [36, 37]). Furthermore, NADP-IDH largely controls CO_2 production in the Krebs cycle (Nicholls and Garland

[27], Walsh and Koshland [49], Williamson and Cooper [52]) not only because it is the more active CO_2-producing enzyme (Fig. 1) but also because it works as a key enzyme in the Sazanov and Jackson substrate cycle in the regulation of Krebs cycle activity (Sazanov and Jackson [42]). In addition, mitochondrial NADP-IDH produces NADPH that is used to produce both, ATP by the electron transport system (ETS), and reduced glutathione (a reactive oxygen species (ROS) scavenger which serves as the cellular defense against oxidative stress-induced damage (Jo et al. [15])). Moreover, cytosolic CO_2-producing NADP-IDH generates NADPH outside the mitochondria, linked to lipid synthesis (Koh et al. [17]), and increases of its activity have been related to hypothyrodism in mammals (Czyzewska et al. [8], Kadenbach et al. [16]). Thus, NADP-IDH measurements may improve the assessment of lipid production on the base of the marine food chain.

Here, we have developed an oceanographic tool based on the $NADP^+$- dependent isocitrate dehydrogenase (NADP-IDH, Eq. 1). We have considered previous studies of NADP-IDH activity in yeast, marine bacteria, and marine fish (turbot) (Berdalet et al. [5], Kornberg and Pricer [18], Munilla-Moran and Stark [25], Munilla-Moran [24], Packard et al. [32], Roy and Packard [39]), and also the development of CO_2-production models based on the measurement NADP-IDH (in this case on the marine bacterium *Pseudomonas nautica* (Packard et al. [32], Roy and Packard [39])). This is the first time NAPD-IDH has been measured in the plankton community. Thus, in order to make this assay sensitive to all its components, we fractionated plankton samples into three separated size-fractions. We measured NADP-IDH activity in the Canarian microplankton (0.7 to 50μm), microzooplankton (50 to 200μm,), and mesozooplankton (200-2000μm). These microplankton samples are mixed communities with heterotrophic organisms (procaryotes, nanoflagellates and also small dinoflagellates) and also autotrophs (cyanobacteria, other eukaryotic picoplankton, autotrophic nanoflagellates and some diatoms) (Schmoker et al. [43]). The microzooplankton community around the Canary Islands is dominated by heterotrophs (large ciliates and dinoflagellates). Finally, Canarian mesozooplankton is also dominated by heterotrophs, largely crustacean copepods (Hernández-León et al. [12]).

In summary, here we propose a new method to assess NAPD-IDH activity in the marine plankton community, and the related potential CO_2 production in order to assess carbon fluxes in the ocean ecosystem. This tool may be also useful in further studies on lipid synthesis in the base of the food chain, and in studies on the ROS scavenging capacity of the marine plankton resources.

2. Material and Methods

In order to develop the NADP-IDH enzyme assay, it was necessary to determine the maximum enzyme activity of the plankton cells, so four main factors need to be specified (Suelter et al. [47]). These are optimum substrate concentration (sections 2.3 and 3.1); optimum pH (sections 2.4 and 3.2); temperature (sections 2.5 and 3.3); and biomass linearity (sections 2.6 and 3.4).In addition, other factors such as the optimum time and speed of centrifugation (sections 2.7 and 3.5); and the stability of the enzyme preparation (sections 2.8 and 3.6), were also assessed to attain the maximum signal. Finally, other factors that impact on the accuracy of the measurement have been included as Supplementary information, such as: sensitivity to different buffer solutions (section 7.1); the extinction coefficient (section 7.2); the assay precision (section 7.6); and the operational issues related to different spectrophotometric responses during the application of the method (section 7.7).

2.1. Plankton sampling procedures

Two zooplankton size fractions (50-200μm and 200-2000μm) were collected from the shallow waters of Sardina del Norte (Gáldar, Gran Canaria island) by three scuba divers dragging a WP2 net horizontally in the upper 10m of the euphotic zone. After being stored in plastic containers during sampling and transport, the samples were fractionated through 2000μm, 200μm, and 50μm nets at laboratory. Then, the zooplankton was carefully removed from the nets with a stainless-steel spatula and stored in 2mL microcentrifuge tubes at -80°C until analysis for less than three months (Ahmed et al. [1]).

Mixed microplankton size fractions (from 0.7 to 50μm) were sampled from Alcaravaneras Beach (Las Palmas de Gran Canaria, Gran Canaria island). Seawater samples were stored in 25L high-density poliethylene (HDPE) containers during sampling and transport and later passed first, through a 50μm net and then through a 0.7μm Glass Fibre Filter (GF/F) in the laboratory. After being blotted to remove excess seawater, all samples were stored, on the GF/F filters, in 2mL microcentrifuge tubes at -80°C until analysis, for less than three months (Ahmed et al. [1]).

2.2. Preparations for kinetic enzyme activity measurements

The 50-200μm and 200-2000μm plankton samples from above, were homogenated in 0.1M phosphate buffer (0.1M Na_2HPO_4, 0.1mM KH_2PO_4, 75μM $MgSO_4 \cdot 7H_2O$, PVP (1.5mg mL^{-1}), TRITON X-100 (2mL L^{-1})) (Supplementary information: Extended information 7.1), by sonication for 45sec at 70% amplitude in a Vibracell VCX 130 Sonics® ultrasonic processor maintained at 0-4°C. The 0.7-50μm plankton samples from above, were homogenized at 0-4°C in the same 0.1M phosphate buffer, with a Teflon® 2mL-pestle PYREX® Potter-Elvehjem tissue grinder at 2600rpm for 2 min. The volume of these homogenates (V_t) must be measured as accurately as possible. Here, it was measured to 50μL. Normally, our homogenate volumes from the zooplankton samples ranged from 1.2 to 15mL, and from the microplankton samples, it ranged from 1.0 to 1.2mL. Crude homogenates were centrifuged in 2mL microcentrifuge tubes at 0-4°C and 4000rpm in an 8.4cm-radius centrifuge rotor (1500 g) for 10 min. NADP-IDH activity was measured kinetically by following the time dependent production of NADPH (Δ_{NADPH}) at 340nm (Δ_{340}) and 18°C in a 1cm plastic cuvette (l) in a Cary 100 U-V visible spectrophotometer for 1000 sec. Note that cuvette temperature should be measured before the assay is initiated, to make sure that the target temperature has been reached within the first 250 sec after the cuvette has been placed into the thermostatted cell holder of the spectrophotometer (Supplementary information: Extended information 7.7). To determine the NADPH concentration ([NADPH]) from the absorbance (A_{340}) of NADPH, we applied the Beer-Lambert law (Eq. 2), using the specific molar extinction coefficient for our reactive solution (ε) (Supplementary information: Extended information 7.2) and the length of the cell (L=1cm).

$$A_{340}=\varepsilon\cdot[\text{NADPH}]\cdot \text{L} \quad (2)$$

So, transposing and using 5.42 absortivity units mL $\mu mol^{-1} cm^{-1}$ for ε we obtained NADPH in $mmol^{-1}$:

$$[\text{NADPH}]=A_{340}/(5.42\cdot L) \quad (3)$$

Thus, in a final volume of 0.5mL of 0.1M phosphate buffer at pH 8.5, different concentrations of $MgCl_2$ (PANREAC 131396), DL-trisodium-isocitrate (SIGMA I1252; which, from here on, we will call isocitrate) and β-$NADP^+$ (SIGMA N0505; which, from here on, we will call $NADP^+$) were added, depending on the aim of each experiment (See sections 2.3,7.1,7.2,2.4, 2.5).

Control assays (blanks) lacked isocitrate. Sequentially, 0.3mL $MgCl_2$ and isocitrate, and 0.1 mL homogenate were added to a 1mL cuvette. The reaction was started by adding 0.1μL $NADP^+$. After 3 min, the linear signal was considered the Δ_{340} related to the IDH activity. Note that this Δ_{340} was linked to the 0.5mL of solution in the cuvette (V_f), of which only 0.1mL was the sample homogenate (V_h, as an aliquot of the total volume of homogenate V_t). To relate the Δ_{340} per mL of the solution of the cuvette to the sample homogenate, we should multiply this value by V_f / V_h (See final expression in Eq.4). Furthermore, this value is generated in absortivity units cm^{-1} sec^{-1}, so, in order to calculate a value in min^{-1} we should multiply it by 60 sec min^{-1} (Eq.4)). Finally, we used an ϵ of 5.42 absortivity units mL μmol^{-1} cm^{-1} (Supplementary information: Extended information 7.2). This calculation is for the production of NADPH per time and mL of homogenate (Δ_{NADPH}) in the cuvette:

Δ_{NADPH} (μmol min^{-1} mL^{-1}) = Δ_{340} (absortivity units cm^{-1} sec^{-1}) $\cdot 60(sec \cdot min^{-1}) \cdot V_f$ (mL) / [5.42 (absortivity units mL $\mu mol^{-1} cm^{-1}) \cdot V_h$(mL)] (4)

where V_f is the final volume in the cuvette (0.5mL in our hands) whereas V_h is the volume of sample homogenate that was added to the cuvette (0.1mL in our hands), so, after applying Eq.4 the NADPH production rate is that related to 1mL of sample homogenate.

Note that, in order to calculate the NADP-IDH activity per mL of sample homogenate, the blank values of the reaction (without DL-trisodium isocitrate, $\Delta_{NADPH-b}$) and the results of the chemical activity among the reagents (same cuvettes with ($\Delta_{NADPH \cdot R}$) and without ($\Delta_{NADPH \cdot R-b}$) DL-trisodium isocitrate, but reacted with 0.1M phosphate buffer instead of homogenated sample) should be subtracted from the total reaction. So the NADP-IDH activity is finally calculated as Eq.5:

NADP-IDH = $\Delta_{NADPH} - \Delta_{NADPH-b} - (\Delta_{NADPH \cdot R} - \Delta_{NADPH \cdot R-b})$(5)

One unit (U) of enzyme activity was defined as the amount of sample able to catalyze the production of 1μmol NADPH in 1 min. However, here, NADP-IDH activity was reported in μmol NADPH min^{-1} (mL of sample homogenate)$^{-1}$ units.

Although in this study we worked directly with the sample homogenate, the natural sample activity can be obtained by multiply that value by the

total volume of the sample-homogenate (V_t)(Eq.6). Finally, if that value is related to an specific volume from an oceanographic region, we can normalise the result by the volume filtered/passed through the zooplankton nets for that sample.

$$\text{NADP-IDH}_{sample} = \text{NADP-IDH}_{homogenate} \cdot V_t \quad (6)$$

where $NADP - IDH_{sample}$ is in μmol of NADPH min^{-1}. Once divided by the filtered ocean volume (e.g. in L units), the activity units is expressed in μmol of NADPH min^{-1} L^{-1} units.

2.3. Kinetic properties of NADP-IDH activity

The affinity between different substrates (or effectors) and the NADP-IDH activity was determined in the three plankton size-fractions (Section 3.2). Their optimum substrate concentrations, their dissociation constants (K_ms) and the NADP-IDH maximum velocity (V_{max}) were calculated from Michaelis-Menten and Hanes-Woolf plots (Suelter et al. [47]). First, enzymatic activity was measured in the same homogenate at pH 8.5, 18°C and ten different concentrations of isocitrate. These ranged from 0.002 to 2.1mM in the cuvette, while maintaining 2mM $MgCl_2$ and 0.3mM $NADP^+$. Second, enzymatic activity was measured in the same homogenate at pH 8.5, 18°C, 2mM $MgCl_2$, 2.1mM isocitrate and ten different concentrations of $NADP^+$, ranging from 0.4 to 400 μM in the cuvette. Finally, enzymatic activity was measured in the same homogenate at pH 8.5, 18°C and at nine different concentrations of $MgCl_2$. These ranged from 0.05 to 12mM in the cuvette, while maintaining 2.1mM isocitrate and 0.3mM $NADP^+$. Results were based on triplicate measurements. In every study, preliminary experiments were performed in order to determine the substrate concentration range needed to optimize the linearisation of the kinetic equations.

We applied three main linearisation techniques to accurately evaluate the K_ms (Supplementary information: Extended information 7.3). Finally, Hanes-Woolf linearisation was accurate to our data base ($p<0.001$ in the whole community). Substrate concentration [S] was plotted against concentration per enzymatic activity ([S]/V). The V_{max} was obtained from the inverse of the slope (a) ($\text{V}_{max} = 1/\text{a}$), whereas K_ms were equal to the ratio of the Y intercept (y_0) and a ($K_m = \text{y}_0/\text{a}$) (Suelter et al. [47]).

2.4. pH studies

The effect of pH on NADP-IDH activity was analysed on mesozooplankton samples (200-2000μm) at 18°C. Different assays were carried out using phosphate buffer at eleven levels of pH that ranged from pH 5.5 to pH 11 (Section 3.2 and Supplementary information: Extended information 7.4). The same buffer solution was maintained for the homogenisation of the samples, the reagent solutions, and the kinetic assay for each pH. The assays were carried out kinetically with 0.2mM $NADP^+$, 2.1mM isocitrate and 2mM $MgCl_2$ in the cuvette. Results were tested in quintuplicate. NADP-IDH activity was reported in μmol NADPH min^{-1}mg $protein^{-1}$ units.

2.5. Temperature studies

The effect of temperature (T) on NADP-IDH activity at pH 8.5 was analysed on mesozooplankton samples of the 200-2000μm size-fractioned plankton community and also on pure NADP-IDH from porcine heart for comparison (I2002, Sigma Aldrich) (Section 3.4). Different assays, following the kinetic procedure, were conducted at nine temperatures ranging from 5 to 60°C. To ensure enzyme specificity, NADP-IDH substrates and cofactors were added to levels of 0.2mM $NADP^+$, 2.1mM isocitrate and 2mM $MgCl_2$ in the spectrophotometer cuvette. Results were based on triplicate measurements of NADP-IDH activity, originally reported in units of μmol NADPH min^{-1}(mL of homogenate)$^{-1}$ units. For Fig.3, results were reported normalised as a percentage of the maximum activity found in the experiment.

The Arrhenius equation describes the dependence of the rate of a chemical reaction on the absolute temperature, as expressed in Eq.7 (Arrhenius [3]):

$$k_{IDH}=A\cdot exp(-E_a/(R\cdot T)) \quad (7)$$

where: k_{IDH} is the NADP-IDH activity related to the temperature in mol NADPH s^{-1}(kg of protein)$^{-1}$; A is the preexponential frequency factor, a unique value, in mol NADPH s^{-1}(kg of protein)$^{-1}$, for each chemical reaction defined by the rate due to collision frequency when reactants are in the correct orientation; Ea is the energy of activation in Kcal mol^{-1}; T is the absolute temperature in ^{o}K and R is the universal molar gas constant in Kcal mol^{-1} ^{o}K^{-1} (1.9872$\cdot$ 10^{-3} Kcal mol^{-1} ^{o}K^{-1}). The Ea and A were obtained from the Arrhenius plot (Fig. 3), where the $\ln(k_{IDH})$ is plotted against 1/T and T

is in 10^{-3} ^{o}K units. Eq.8 describes the linear regression from this Arrhenius plot (y=a·x +y_0), where x is 1/T and y_0 is ln(k_{IDH}):

$$\ln(k_{IDH})=\ln(A)-(E_a/R)\cdot(1/T) \quad (8)$$

E_a is related to the slope (a) of this linear regression, so a=-E_a/R. A is obtained from the intercept on the y axis (y_0=ln(A)). The enthalpy of activation (ΔH^*), in Kcal mol^{-1}, was calculated from the E_a as represented on Eq.9 (Low et al. [19]):

$$\Delta H^*=E_a-R\cdot T \quad (9)$$

Here, R is $1.9872\cdot10^{-3}$ Kcal mol^{-1} ^{o}K^{-1}, as above, and T is the standard temperature of 25^{o}C, expressed in ^{o}K (298^{o}K).

2.6. Biomass linearity and limit of detection

The biomass linearity was tested on the 0.7-50μm and the 200-2000μm samples by diluting them (Section 3.4). This resulted in seven solutions ranging from 5% (4μg of proteins mL^{-1}) to 100% (83μg of proteins mL^{-1}) of the natural sample in the case of the microplankton and nine solutions, ranging from 0.39% (3μg of proteins mL^{-1}) to 100% (684μg of proteins mL^{-1}) of the natural sample for the mesozooplankton.

The activity was measured at 18^{o}C, with the optimum pH and ligands from previous experiments (pH 8.2, 6mM $MgCl_2$, 2.1mM isocitrate and 0.3mM $NADP^+$). The assessment of the limit of detection was done by comparison of the NADP-IDH activity (in μmol NADPH min^{-1} mL^{-1} units) and the proteinaceus biomass (mg protein mL^{-1} units). Also a comparison of the percentage of the NADP-IDH activity and the percentage of dilution is included for both the microplankton and the mesozooplankton samples.

2.7. Centrifugation studies

Centrifugation is used to separate cell membranes and organelles from the cytosol. It clarifies the enzyme preparation and increases the assay sensitivity. The effect of centrifugation on NADP-IDH activity was analysed on mesozooplankton samples and microplankton samples at pH 8.5 and 18°C. In the cuvette, 0.2mM $NADP^+$, 0.2mM NAD^+, 2.1mM isocitrate and 2mM $MgCl_2$ were used to ensure the enzymatic activity (Section 3.5). Five assays

were conducted: (1) without centrifugation, where the activity was measured after 8min of gravitational sinking (an average of 8min was needed before maintaining a constant absorbance at 500nm in zooplankton samples, which decreased during the sinking of particles in the cuvette); (2) centrifugation of the samples during 2min at 1000 rpm (at 375 g); (3) centrifugation of the samples during 2min at 2000rpm (at 750 g); (4) centrifugation of the samples during 2min at 4000rpm (at 1500 g); (5) centrifugation of the samples during 10min at 4000 rpm (at 1500 g). Results were tested in quintuplicate. NADP-IDH activity was reported in μmol NADPH min^{-1}(mL of homogenate)$^{-1}$ units and normalized by V_{max} as a percentage.

2.8. Stability of the enzyme preparation from mysid samples

As an application of this methodology, we assayed the NADP-IDH on Mysidacea samples. Mysidacea (*Leptomysis lingvra*) were collected from the shallow waters of Taliarte (Telde, Gran Canaria island) by two scuba divers with an 8″ fish net, close to the bottom. After being stored in plastic containers during sampling and transport, the organisms were gently captured by using 3mL plastic pipettes, and stored in 2mL microcentrifuge tubes at -80°C until analysis.

The samples were homogenised as explained in Subsection 2.2 for the 200-2000μm size-fractionated zooplankton samples. In order to assess the loss of NADP-IDH activity per time after the homogenisation, the homogenate was maintained on ice during the whole experiment. The activity was measured at 18ºC, with the optimum pH and ligands from previous experiments (pH 8.2, 6mM $MgCl_2$, 2.1mM isocitrate and 0.3mM $NADP^+$). NADP-IDH activity was tested in triplicates, every 90min, for 8h; and was reported in μmol NADPH min^{-1}(mL of homogenate)$^{-1}$ units and normalised by V_{max} as a percentage (Section 3.6).

2.9. Biomass

Biomass was determined from samples kept for enzyme activities by the protein method of Lowry *et al.* (1951) Lowry et al. [20] modified by Rutter (1967) Rutter [40] using bovine serum albumin (BSA) as standard. Biomass was reported in mg of protein.

2.10. Statistics of the substrate and temperature kinetics

In the kinetic properties studies (Section 2.3 and 3.2), F test was used to determine the difference among the logarithmically transformed (lnV vs

ln[S]) Michaelis-Menten curves from three size-fractionated samples (Pentecost [35]). F test was also used to determine the difference between the Arrhenius plots related to the plankton and pure porcine samples (Section 2.7 and 3.4). The difference between the regression coefficients of the Arrhenius plots was analysed via t test (Sachs [41]).

Table 1: Summary of the symbols used to identify the equation parameters. D.M. means that this parameter can be obtained by direct measurements.

Parameter	Definition	Source
ΔNADPH	$[NADPH]$ increase per time	D.M., Eq.4, 5
Δ340	A_{340} increase per time of the absorbance at 340nm	D.M., Eq.4
$\boldsymbol{V_f}$	Final volume in the cuvette	D.M., Eq.4
$\boldsymbol{V_h}$	Volume of the sample-homogenate added into the cuvette	D.M., Eq.4
$\boldsymbol{V_t}$	Volume of the total sample-homogenate	D.M., Eq.6
ΔNADPH-b	$[NADPH]$ increase per time without adding isocitrate	D.M., Eq.5
ΔNADPH·R	$[NADPH]$ increase per time without adding sample	D.M., Eq.5
ΔNADPH·R-b	$[NADPH]$ increase per time without adding sample neither isocitrate	D.M., Eq.5
$\boldsymbol{A_{340}}$	Absorbance at 340nm	D.M., Eq.2, 3
ϵ	Extinction coefficient	Eq.4, 2, 3
$\mathbf{k}_{IDH}$	NADP-IDH activity related to temperature	Eq.7, 8
$\boldsymbol{A}$	Preexponential frequency factor	Eq.7, 8
Ea	Energy of activation	Eq.7, 8, 12, 13, 14
R	Universal molar gas constant	Eq.7, 8, 9, 12, 13, 14
T	Temperature	D.M., Eq.7, 8, 9
ΔH*	Enthalpy of activation at standard conditions	Eq.9
UsIDH	Theoretical units of IDH	Eq.16
UmIDH	Measured units of IDH	D.M., Eq.16
$\mathbf{V}_{max}$	Maximum velocity of an enzyme-catalised reaction	D.M., Eq.11
Km	Michaelis-Menten constant	D.M., Eq.11, Table 2
[S]	Substrate concentration	Eq.11
$\mathbf{K}_1$	Velocity constant at T1	D.M. and Eq.12, 13, 14
$\mathbf{K}_2$	Velocity constant at T2	D.M., Eq.12, 13, 14
NADP-IDH(Ti)	NADP-IDH activity at in-situ T	D.M. and Eq.10
NADP-IDH(Tm)	NADP-IDH activity at T during measurement	D.M. and Eq.10
$\mathbf{T}_i$	In-situ temperature	D.M. and Eq.10
$\mathbf{T}_m$	Inside-cuvette temperature during measurement	D.M. and Eq.10

3. Results

3.1. Kinetic properties

Specific concentrations of substrate, cofactor and effector need to be determined both to understand their affinity with the enzyme, and to optimize the conditions of the enzyme assay. Thus, NADP-IDH kinetic constants in plankton size-fractionated samples were calculated from Michaelis-Menten plots (Fig.2 and Supplementary information: Extended information 7.3, Tables 1, 2, 3, 4, 5, 6, 7, 8 and 9). The average K_ms for the community were 232±34μM for isocitrate, and 22±7μM for $NADP^+$ (Table 2). These results were consistent with those arisen by Hannes-Wolf linearisations, 271±63μM for isocitrate, and 18±3μM for $NADP^+$ (Supplementary information: Extended information 7.3, Table 10).

Table 2: Michaelis-Menten hyperbolic curves for isocitrate and $NADP^+$ affinity in marine plankton samples. K_m is in mM units.

Size-fractionated sample / Substrate	**a (%V_{max})**	**y_0 (K_m)**	**r^2**	***p*-value**
200-2000μm / isocitrate	109.34	0.225	0.987	<0.0001
50-200μm / isocitrate	109.25	0.270	0.985	<0.0001
0-7-50μm / isocitrate	96.99	0.203	0.962	<0.0001
Average values for isocitrate	105.20	0.232±0.034	NA	NA
200-2000μm / $NADP^+$	102.75	0.024	0.926	<0.0001
50-200μm / $NADP^+$	93.45	0.023	0.930	0.0001
0-7-50μm / $NADP^+$	96.83	0.020	0.981	<0.0001
Average values for $NADP^+$	97.68	0.022±0.007	NA	NA

The optimal values to measure NADP-IDH activity (100% V_{max} in Fig.2) in this community are 2mM for isocitrate and 0.3mM for $NADP^+$ (Fig.2). By inspection of Fig.2c, we conclude that, although 4mM of $MgCl_2$ would be enough to reach the V_{max} in the 50-2000μm fractions, an optimal value of 6mM for $MgCl_2$, is needed to ensure that all the community reaches 100%V_{max}. This dependence on $MgCl_2$ in the first mM of $MgCl_2$ takes a sigmoid shape (average r^2=0.985 from all the size fractioned data, Supplementary information: Tables 7, 8 and 9). This is likely due to a positive cooperative effect according to the definition by Dixon and Webb (1964) (Dixon and Webb [10]), where at least a minimum concentration of Mg^{2+} (0.3mM in our hands) is needed to begin the enzymatic reaction.

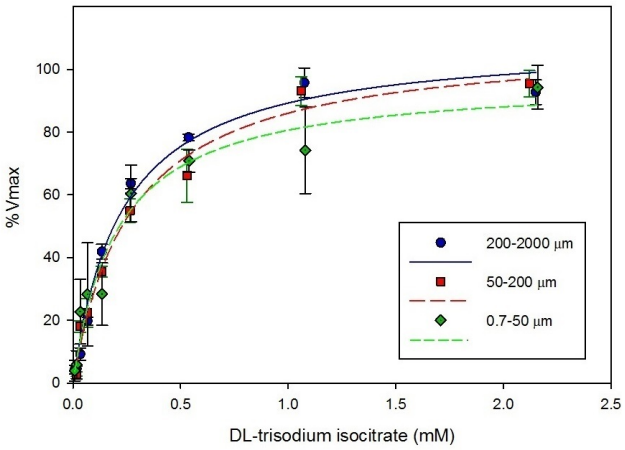

(a) Affinity between NADP-IDH and isocitrate

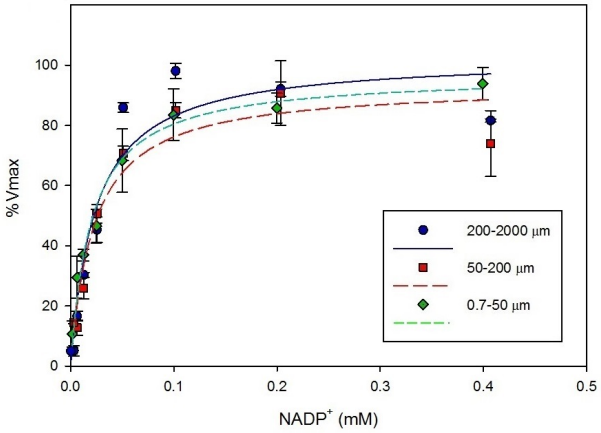

(b) Affinity between NADP-IDH and $NADP^+$

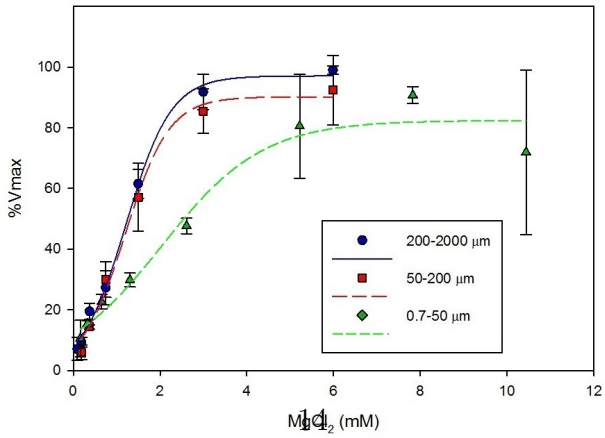

(c) Affinity between NADP-IDH and Mg^{2+}

Figure 2: Michaelis-Menten plots to determine the NADP-IDH K_m and optimum values for isocitrate, $NADP^+$ and Mg2+ for different plankton community size fractions.

3.2. Effect of pH

The effect of pH on the catalytic activity of the NADP-IDH was measured on phosphate buffer at 18ºC, with the same concentration of ligands. In our hands, the maximum activity was obtained at pH 8.19 (Supplementary information: Fig.10), whereas measurements below pH 7.62 and above pH 8.75 led to activities lower than 50% of its V_{max} (pKas) (Supplementary information: Extended information 7.4, Tables 11 and 12).

3.3. Effect of Temperature

The relationship between NADP-IDH activity and temperature was studied on the poikilothermic 200-2000 μm samples and compared to the results on homoeothermic porcine-heart pure NADP-IDH (Fig.3). Both activities increased with temperature following an Arrhenius relationship before reaching an optimum temperature, 27.6ºC on the poikilothermic subtropical plankton samples (Supplementary information: Table 13), and 38.6ºC on the homoeothermic porcine-heart pure NADP-IDH ones (Supplementary information: Table 14). At higher temperatures, the activity decreased. Besides, the Q_{10} between 15ºC and 25ºC was 1.98 for the zooplankton 200-2000μm size-fractioned marine samples. Although this value is higher than the NADP-IDH reported by Munilla-Moran on turbot larvae between 20-35ºC (1.74) (Munilla-Moran [24]), it is consistent with the Q_{10} for respiratory rates in epipelagic marine copepods (1.8-2.1) (Ikeda et al. [14]). From this data set, the Arrhenius energy of activation (Ea) had a value of 20.4 Kcal mol^{-1} for the poikilothermic subtropical plankton samples and 21.40 Kcal mol^{-1} for the homoeothermic pure enzyme from porcine heart; the Arrhenius frequency factor (A) was $2.19{\cdot}10^{11}$ mol NADPH s^{-1} (kg of protein)$^{-1}$ for the plankton samples and $1.60{\cdot}10^{13}$ for the porcine heart pure NADP-IDH; and finally, the Arrhenius enthalpy of activation at 25ºC (ΔH^*) was 19.81 Kcal mol^{-1} for the plankton samples and 20.76 Kcal mol^{-1} for the porcine heart NADP-IDH. These results suggested that, for NADP-IDH, although the frequency factor (A) was different (F test, $F_{(2,37)}$=4.64, p=0.05), Ea and ΔH^* were not significantly different between the two types of organisms (t test, $t(39)$=0.0773, p=0.05).

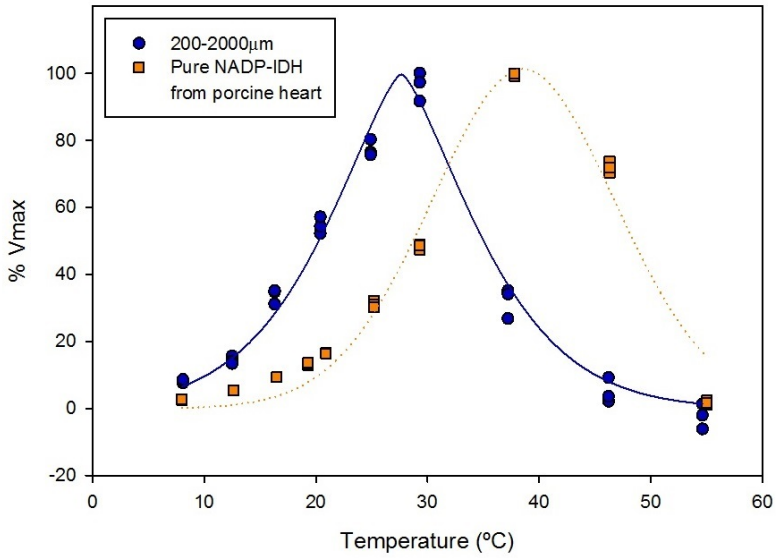

(a) Temperature impact on NADP-IDH activity.

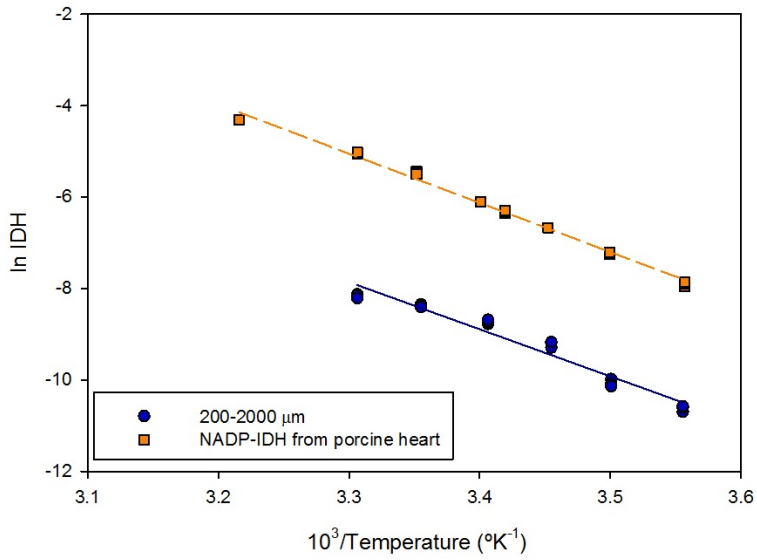

(b) Arrhenius plot.

Figure 3: Temperature dependence of NADP-IDH activity (Supplementary information: Tables 13 and 14).

This permits the development of a common Arrhenius equation. When the in-situ T(T_i) is different from T during the assay (T_m), the NADP-IDH activity needs to be converted. The in-situ activity (NADP-IDH(T_i)) results by the use of the Arrhenius equation, combined with Van't Hoff equation (Atkin and de Paula [4], Supplementary information: Extended information 7.5), based on Arrhenius *Ea*, as expressed on Eq.10:

$$\text{NADP-IDH}(T_i)=\text{NADP-IDH}(T_m)\cdot exp((20.39/R)\cdot(1/T_m\text{-}1/T_i)) \quad (10)$$

where: NADP-IDH(T_i) is NADP-IDH activity at in-situ temperature; NADP-IDH(T_m) is NADP-IDH activity at temperature in the spectrophotometric cuvette during measurement; R is $1.9872{\cdot}10^{-3}$ Kcal mol^{-1} $^oK^{-1}$; T_m is temperature in the spectrophotometric cuvette during measurement in ^{o}K; and T_i in-situ temperature in ^{o}K.

3.4. Biomass linearity and limit of detection

Once we applied the optimum conditions, the NADP-IDH resulted a measurement with an standard deviation less than 3.5% on every ten duplicates (Supplementary information: Extended information 7.6 and Tables 18 and 19), when samples are within the limit of detection. To accurately determine this limit, we measured NADP-IDH in seven different dilutions of both 200-2000μm and 0.7-50μm homogenates. The linearity of Fig.4, shows that samples can be diluted without changing the relationship between NADP-IDH and biomass (a>0.95 in both sample types (p<0.0001)) (Supplementary information: Table 20).

Biomass in the 200-2000μm original homogenates was 0.68±0.12mg protein mL^{-1} while 0.7-50μm biomass was 0.08±0.02mg protein mL^{-1}. The limit of detection for 200-2000μm samples was 3±0.02μg protein mL^{-1} and for 0.7-50μm samples it was 4± 0.06μg protein mL^{-1}. Thus, homogenates more concentrated than 50μg protein mL^{-1} for 200-2000μm plankton size samples, and than 25μg protein mL^{-1} for 0.7-50μm size sample are needed to apply this method.

For 0.7-50μm samples under oligotrophic conditions, this biomass is reached after filtering 4L through the 0.7 GF/F glass fibre filters, whereas during eutrophic conditions, 2.5L were enough. In deep water samples, we assume that more volume would be required (10L or even 20L) to stay above the limit of detection. For unknown conditions, and also for 50-2000μm samples, we suggest to make preliminary measurements to adjust both the filtered

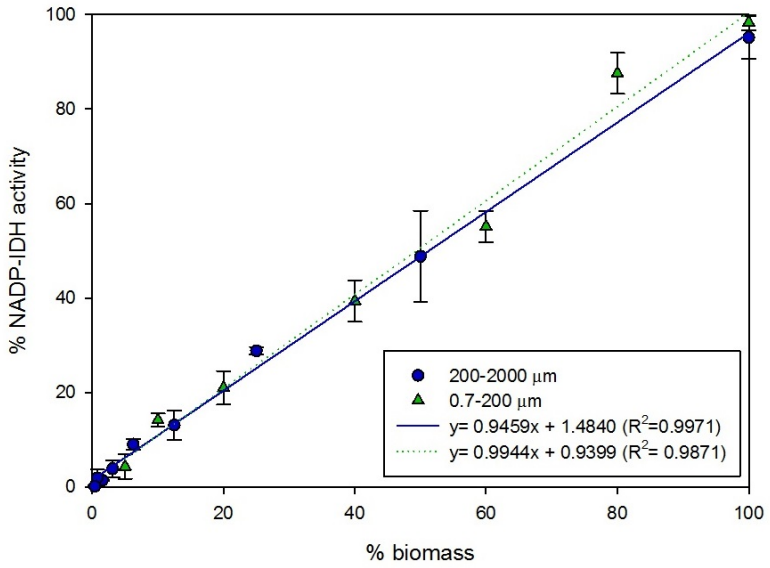

Figure 4: Biomass linearity of marine-plankton NADP-IDH in 0.7-50 and 200-2000 μm samples, % of dilution (Supplementary information: Table **??**).

ocean volume of the sample and the total volume of sample-homogenate (see Section 2.2) to the biomass of the specific oceanographic region.

3.5. Effect of centrifugation

GF/F filtered samples (0.7-50μm, green columns in Fig.5) need strong centrifugation (1500g) to achieve the maximum NADP-IDH activity with the lowest standard deviation (12.6 % of the activity). Note that no signal is obtained without centrifugation, due to the turbidity of the filter fibres.

On the other hand, sonicated samples (200-2000μm, blue columns in Fig.5) are negatively affected by centrifugation. However, part of the activity reached without centrifugation is related to a negative blank, which may indicate either other enzymes are consuming NADPH, or that particle sinking interfered with the signal. As both problems are solved by centrifugation, we argue that at least 375g are required for sonicated samples.

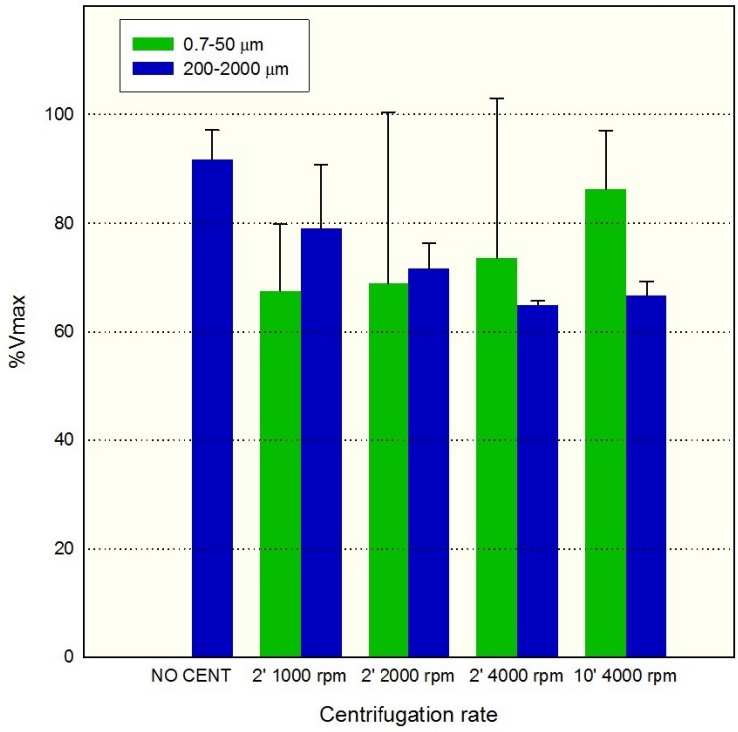

Figure 5: Centrifugation effects on NADP-IDH activity. Note that, in our hands: 1000rpm equaled 375g; 2000rpm equaled 750g; and 4000rpm equaled 1500g

3.6. Stability of the enzyme preparation from mysid samples

NADP-IDH dropped continuously per time (Fig.6) during the 500min measurements. A regression coefficient of 0.109 (r^2=0.9771, p<0.0001) suggests an average lost of 1.1% of NADP-IDH activity per 10min. This means that only 3% of the activity is lost if analyses are confined to the first half-hour after centrifugation.

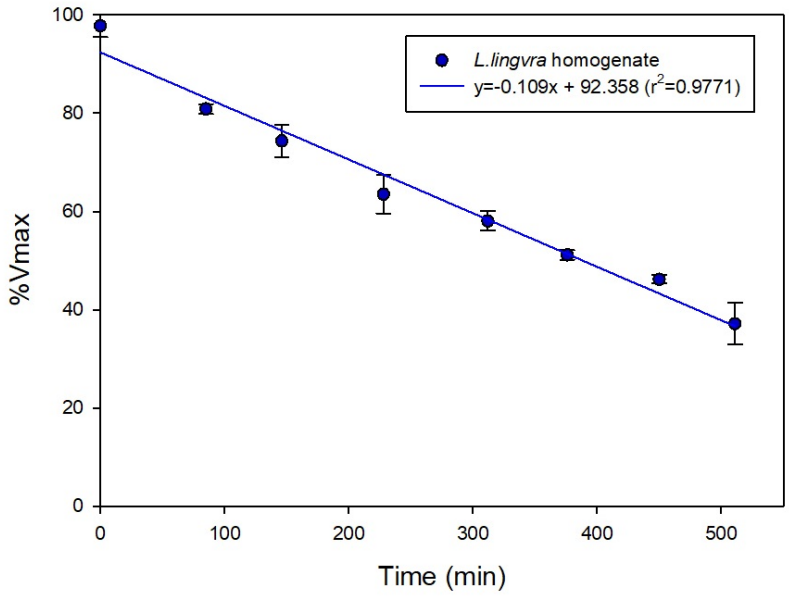

Figure 6: Stability of the enzyme preparations from *L. lingvra* samples (see Supplementary information Table 22). T_0 is the end of the centrifugation process.

4. Discussion

4.1. What does the development of the assay reveal about plankton NADP-IDH?

While determining the conditions for assaying the V_{max} of NADP-IDH, we also determined the K_m for isocitrate and $NADP^+$ (Fig. 2, Supplementary information: Extended information 7.3). Based on this type of proxy, other studies have developed mathematical models, pioneered on bacteria, to determine the physiological (R_{CO2}) (Roy and Packard [39], Packard et al. [32]). Thus, further models based on NADP-IDH measurements and combined with the in-cell concentrations of isocitrate and $NADP^+$ on marine plankton samples may result on marine physiological (R_{CO2}) measurements at high acquisition rates. Besides, after the isolation of mitochondria from cytosol (Wieckowski et al. [51]), mitochondrial NADP-IDH measurements may serve as a proxy of the ROS scavenging capacity of the cells (Jo et al. [15]). Accordingly, cytosolic NADP-IDH measurements may facilitate the assessment of lipid synthesis in the base of the marine food chain (Koh et al. [17]).

On marine plankton samples, NADP-IDH measurements should be done maintaining the buffer, pH levels, and the Arrhenius relationship developed in this study. If these conditions are changed, the K_ms would need to be reassessed (Olano et al. [28]). In our hands, both the isocitrate and $NADP^+$ K_ms were up to one order of magnitude higher than other reported values Munilla-Moran [24]. These differences can be attributed to our specific chemical conditions (buffer, pH, T) that are likely responsible for the variations in the affinity between enzymes and their substrates (Olano et al. [28]) .

Michaelis-Menten constants are affected by pH levels that impact ionisation around the enzyme active site. Our results, with an optimum pH of 8.2 (section 3.2), are consistent with those reported in turbot larvae (optimum pH between 7.8 and 9.0) (Munilla-Moran [24]). The pK_as of 7.62 and 8.75, which are close to the optimum value, indicate a high enzyme sensitivity to pH changes. As the pH involved in the reaction is intracellular, it is controlled by cellular membranes so slight environmental pH changes are unlikely to affect the intracellular enzymatic activity (Simčič and Brancelj [44]). However, the influence of pH on the metabolic response (in the short, medium and long term) of the plankton community should be assessed in further research, particularly in the current scenario of increasing ocean acidification.

Another key factor that impacts enzyme kinetics is temperature (T). The NADP-IDH activity in the subtropical plankton drops as T rises above 27.6ºC, whereas in pure NADP-IDH from porcine heart, this occurs above 38.6ºC. This decreasing activity can be related: (1) to denaturation of the enzyme; (2) to a direct effect of T on the collision history at any stage of the reaction (formation of the enzyme-substrate complex; conversion of the enzyme-product complex; or dissociation of the product); (3) or to the ionisation of the different groups comprising the active site. This will change the substrates' K_ms even under the same pH conditions (Dixon and Webb [10]). Under a global warming scenario, further research on the T effects on plankton metabolism and the biochemical response will improve our knowledge about the magnitude and reversibility of the negative high-temperature effects on respiratory metabolism and physiology. These future studies will be relevant for poikilotherms, taking into account that environmental temperatures higher than the optimum (30-35ºC for subtropical plankton) will affect the enzymatic structure that supports the metabolism of these organisms. High-latitude plankton community, likely with a lower optimum T, should be particularly studied. In the case of homoeothermic samples (from porcine heart) the optimum T is around ten degrees higher than in poikilothermic samples. However, *Ea* and ΔH^* are not significantly different, being also consistent with *Ea* reported by Munilla-Moran for NADP-IDH in turbot (around 23.5 Kcal mol^{-1} on turbot liver and 23.3 Kcal mol^{-1} for turbot larvae) and by Moon and Hochachaka for cold-adapted and warm-adapted NADP-IDH in rainbow-trout liver (18 Kcal mol^{-1}) (Munilla-Moran [24], Munilla-Moran and Stark [25], Moon and Hochachka [22]). Thus, although there seems to be an adaptation to homoeothermic conditions allowing high activity at higher temperatures, a common basic structure seems to have been maintained even after differences in evolution.

4.2. Why should this metabolic assay be measured kinetically?

While studying enzyme activities, two approaches can be used: (1) Two point measurements (endpoint); and (2) time-course monitoring (kinetics). Endpoint measurements are only feasible, with reliable results, when the reaction is linear, and this condition must be frequently validated (Škorjanc and Pette [45]) unless the behaviour of the sample is well-known. Here, all measurements were made kinetically, and even though the linear relationship was well maintained for more than 1000s, we realise that some conditions, such as low and high biomass samples, the lag until thermal equilibrium in the

cuvette, or the blank signalling may change the linearity of the reaction (see Supplementary Information: Extended information 7.7), rendering endpoint detection unsuitable. From these different observations we conclude that by measuring the A_{340} kinetics for 1000 seconds, the NAPD-IDH activity can be determined with confidence. This time-course analysis demonstrates the impact of pH, T, dilution, substrate concentration, biomass and centrifugation (see Supplementary Information: Extended information 7.7). This visualisation, not detected by end-point approach, lends itself to modifying assay conditions when needed. Thus, we recommend using kinetics for measuring NADP-IDH in oceanographic research.

5. Conclusions

- An enzyme assay for IDH (NADP-IDH) in zooplankton and microplankton has been developed. It is based on the reduction of $NADP^+$ in 0.1M phosphate buffer, 6mM $MgCl_2$, 2mM of isocitrate and 0.3mM $NADP^+$, at a pH of 8.2. The assay has a temperature optimum at 30°C.

- In our hands, the apparent Km values for the substrates were 232±34 μM for isocitrate and 22±7 μM for $NADP^+$. To make these NADP-IDH measurements on marine plankton samples we recommended maintaining the buffer, pH levels, and the Arrhenius relationship developed in this study. If these conditions are changed, the K_ms would need to be reassessed.

- The rates of NADPH per min and per mL of homogenate (μmol NADPH min^{-1} mL^{-1}) are obtained kinetically by following the increase of absorbance at 340nm (the slope, Δ_{340}). Activities are converted to μmol of NADPH by a molar extinction coefficient of 5.42 mL $\mu mol^{-1} cm^{-1}$. However, we suggest that new investigators verify the ε in their own solutions and laboratory conditions. This practice will reduce error.

- We recommend using kinetic analysis for measuring NADP-IDH. This time-course analysis demonstrates the impact of pH, T, dilution, substrate concentration, biomass and centrifugation. This visualisation lends itself to modifying assay conditions when needed as well as insuring against non-linearity.

- Temperature experiments confirmed a clear Arrhenius relationship between NADP-IDH activity and T, in both poikilothermic and homeothermic samples, with similar *Ea* for mesozooplankton samples (20.4 Kcal mol^{-1}) and for porcine heart NADP-IDH (21.4 Kcal mol^{-1}).

- The methodology presented in this study measures accurately the NADP-IDH activity in plankton community. This is a basic measurement that will allow the development of an oceanographic tool to assess CO_2 production in the marine water column.

- After the isolation of mitochondria from cytosol, this tool also allows the measurement of both mitochondrial and cytosolic NADP-IDH in marine plankton. Mitochondrial NADP-IDH may be used to assess the ROS scavenging capacity of plankton communities while cytosolic NADP-IDH may be used as a proxy of the lipid production at the base of the marine food chain.

6. Acknowledgements

We are grateful to D.Ortega, G.Muntaner, R.Pérez, A.Marrero, M.Grau, R.Triay-Portella and E.Bru for their help with the living samples. Thanks are also extending to A.Tames, M.Espinosa, G.Martinez-Uribe, A.Rueda-Duran, J.Coca and F.Betancort for their support and encouragement to the complete development of this study. This work was funded by project BIOMBA awarded to M.G by the Spanish Ministry of Economy and Competitiveness (CTM2012-32729-MAR). M.T-E received financial support from University of Las Palmas de Gran Canaria (PIFULPGC-2013-CIENCIAS-1). T.T.P was largely supported by TIAA-CREF and Social Security (USA) but also partially by Canary Islands CEI: Tricontinental Atlantic Campus. This work was completed while M.T-E was a Ph.D. student in the ULPGC Doctoral Programme in Oceanography and Global Change.

References

References

[1] Ahmed, S., Kenner, R., King, F.. Preservation of enzymic activity in marine plankton by low-temperature freezing. Marine Chemistry 1976;4(2):133–139.

[2] Alp, P.R., Newsholme, E.A., Zammit, V.A.. Activities of citrate synthase and NAD^+-linked and $NADP^+$-linked isocitrate dehydrogenase in muscle from vertebrates and invertebrates. Biochemical Journal 1976;154(3):689–700.

[3] Arrhenius, S.. Über die reaktionsgeschwindigkeit bei der inversion von rohrzucker durch säuren. Zeitschrift für physikalische Chemie 1889;4(1):226–248.

[4] Atkin, P., de Paula, J.. Atkins' physical chemistry. WH Freeman and Company Books 2006;:p747–755.

[5] Berdalet, E., Packard, T., Lagace, B., Roy, S., St-Amand, L., Gagné, J.P.. CO_2 production, O_2 consumption and isocitrate dehydrogenase in the marine bacterium *Vibrio natriegens*. Aquatic microbial ecology 1995;9(3):211–217.

[6] Berggren, M., Lapierre, J.F., Del Giorgio, P.A.. Magnitude and regulation of bacterioplankton respiratory quotient across freshwater environmental gradients. The ISME journal 2012;6(5):984–993.

[7] Colman, R.F.. Mechanisms for the oxidative decarboxylation of isocitrate: implications for control. Advances in enzyme regulation 1975;13:413–433.

[8] Czyzewska, U., Tylicki, A., Siemieniuk, M., Strumilo, S.. Changes of activity and kinetics of certain liver and heart enzymes of hypothyroid and T 3-treated rats. Journal of physiology and biochemistry 2012;68(3):345–351.

[9] Denton, R.M., Richards, D.A., Chin, J.G.. Calcium ions and the regulation of NAD^+-linked isocitrate dehydrogenase from

the mitochondria of rat heart and other tissues. Biochemical Journal 1978;176(3):899.

[10] Dixon, M., Webb, E.C.. Enzymes, Third edition, 1979.

[11] Gálvez, S., Gadal, P.. On the function of the NADP-dependent isocitrate dehydrogenase isoenzymes in living organisms. Plant Science 1995;105(1):1–14.

[12] Hernández-León, S., Gomez, M., Arístegui, J.. Mesozooplankton in the Canary Current System: The coastal–ocean transition zone. Progress in Oceanography 2007;74(2):397–421.

[13] Hernández-Leon, S., Gómez, M., et al. Factors affecting the respiration/ETS ratio in marine zooplankton. Journal of Plankton Research 1996;18(2):239–255.

[14] Ikeda, T., Kanno, Y., Ozaki, K., Shinada, A.. Metabolic rates of epipelagic marine copepods as a function of body mass and temperature. Marine Biology 2001;139(3):587–596.

[15] Jo, S.H., Son, M.K., Koh, H.J., Lee, S.M., Song, I.H., Kim, Y.O., Lee, Y.S., Jeong, K.S., Kim, W.B., Park, J.W., et al. Control of mitochondrial redox balance and cellular defense against oxidative damage by mitochondrial $NADP^+$-dependent isocitrate dehydrogenase. Journal of Biological chemistry 2001;276(19):16168–16176.

[16] Kadenbach, B., Goebell, H., Klingenberg, M.. Differential action of thyroid hormones on enzyme levels of the DPN and TPN specific isocitrate dehydrogenase. Biochemical and biophysical research communications 1964;14(4):335–339.

[17] Koh, H.J., Lee, S.M., Son, B.G., Lee, S.H., Ryoo, Z.Y., Chang, K.T., Park, J.W., Park, D.C., Song, B.J., Veech, R.L., et al. Cytosolic $NADP^+$-dependent isocitrate dehydrogenase plays a key role in lipid metabolism. Journal of Biological Chemistry 2004;279(38):39968–39974.

[18] Kornberg, A., Pricer, W.. Di-and triphosphopyridine nucleotide isocitric dehydrogenases in yeast. Journal of Biological Chemistry 1951;189(1):123–136.

[19] Low, P.S., Bada, J.L., Somero, G.N.. Temperature adaptation of enzymes: roles of the free energy, the enthalpy, and the entropy of activation. Proceedings of the National Academy of Sciences 1973;70(2):430–432.

[20] Lowry, O.H., Rosebrough, N.J., Farr, A.L., Randall, R.J., et al. Protein measurement with the folin phenol reagent. Journal of Biological Chemistry 1951;193(1):265–275.

[21] Mayzaud, P., Boutoute, M., Gasparini, S., Mousseau, L., Lefevre, D.. Respiration in marine zooplankton—the other side of the coin: CO_2 production. Limnology and oceanography 2005;50(1):291–298.

[22] Moon, T.W., Hochachka, P.. Temperature and enzyme activity in poikilotherms. isocitrate dehydrogenases in rainbow-trout liver. Biochemical Journal 1971;123(5):695–705.

[23] Morris, J., Redfearn, E.. Vitamins and coenzymes. In: Data for Biochemical Research. Clarendon Press Oxford; 1969. p. 123–167.

[24] Munilla-Moran, R.. Biochemical studies in marine species—II. $NADP^+$-dependent isocitrate dehydrogenase from turbot (*Scophthalmus maximus L.*) larvae. Comparative Biochemistry and Physiology Part B: Comparative Biochemistry 1994;107(1):61–68.

[25] Munilla-Moran, R., Stark, J.. Biochemical studies in marine species—I. $NADP^+$-dependent isocitrate dehydrogenase from turbot liver (*Scophthalmus maximus L.*). Comparative Biochemistry and Physiology Part B: Comparative Biochemistry 1989;93(4):823–828.

[26] Nelson, D.L., Cox, M.M.. Lehninger principles of biochemistry, Fifth Edition. W.H. Freeman and Company, 2008.

[27] Nicholls, D., Garland, P.. The control of isocitrate oxidation by rat liver mitochondria. Biochemical Journal 1969;114(2):215–225.

[28] Olano, J., de Arriaga, D., Busto, F., Soler, J.. Kinetics and thermostability of NADP-isocitrate dehydrogenase from *Cephalosporium acremonium*. Applied and environmental microbiology 1995;61(6):2326–2334.

[29] Osma, N., Fernández-Urruzola, I., Packard, T., Postel, L., Gómez, M., Pollehne, F.. Short-term patterns of vertical particle flux in northern Benguela: a comparison between sinking POC and respiratory carbon consumption. Journal of Marine Systems 2014;140:150–162.

[30] Osma, N., Maldonado, F., Fernández-Urruzola, I., Packard, T.T., Gómez, M.. Variability of respiration and pyridine nucleotides concentration in oceanic zooplankton. Journal of Plankton Research 2016;38(3):537. doi:10.1093/plankt/fbw001.

[31] Packard, T.. The measurement of respiratory electron transport activity in marine phytoplankton. Journal of Marine Research 1971;29(3):235–244.

[32] Packard, T., Berdalet, E., Blasco, D., Roy, S., St-Amand, L., Lagacé, B., Lee, K., Gagne, J.. CO_2 production predicted from isocitrate dehydrogenase activity and bisubstrate enzyme kinetics in the marine bacterium *Pseudomonas nautica*. Aquatic Microbial Ecology 1996;11(1):11–19.

[33] Packard, T.T., Codispoti, L.. Respiration, mineralization, and biochemical properties of the particulate matter in the southern Nansen Basin water column in April 1981. Deep Sea Research Part I: Oceanographic Research Papers 2007;54(3):403–414.

[34] Packard, T.T., Gómez, M.. Modeling vertical carbon flux from zooplankton respiration. Progress in Oceanography 2013;110:59–68.

[35] Pentecost, A.. Analysing environmental data. Prentice Hall, 1999.

[36] Plaut, G.W.. DPN-linked isocitrate dehydrogenase of animal tissues. Curr Top Cell Regul 1970;2:1–27.

[37] Plaut, G.W.E.. Isocitric dehydrogenase (TPN-linked) from pig heart (revised procedure); New York: Academic Press; volume V of *Methods in Enzymology*. p. 645–651. X.

[38] Romero-Kutzner, V., Packard, T.T., Berdalet, E., Roy, S., Gagné, J.P., Gómez, M.. Respiration quotient variability: bacterial evidence. Marine Ecology Progress Series 2015;519:47–59.

[39] Roy, S., Packard, T.. CO_2 production rate predicted from isocitrate dehydrogenase activity, intracellular substrate concentrations and kinetic constants in the marine bacterium *Pseudomonas nautica*. Marine Biology 2001;138(6):1251–1258.

[40] Rutter, W.. Protein determination in embryos. In: Methods in developmental biology. Crowell New York; 1967. p. 671–683.

[41] Sachs, L.. Applied statistics: a handbook of techniques. Springer Science & Business Media, 2012.

[42] Sazanov, L., Jackson, J.. Proton-translocating transhydrogenase and NAD-and NADP-linked isocitrate dehydrogenases operate in a substrate cycle which contributes to fine regulation of the tricarboxylic acid cycle activity in mitochondria. FEBS letters 1994;344(2-3):109–116.

[43] Schmoker, C., Hernández-León, S., Calbet, A.. Microzooplankton grazing in the oceans: impacts, data variability, knowledge gaps and future directions. Journal of Plankton Research 2013;35(4):691–706.

[44] Simčič, T., Brancelj, A.. Effects of pH on electron transport system (ETS) activity and oxygen consumption in *Gammarus fossarum*, *Asellus aquaticus* and *Niphargus sphagnicolus*. Freshwater Biology 2006;51(4):686–694.

[45] Škorjanc, D., Pette, D.. Kinetic versus endpoint measurement for quantitative histochemical determination of enzyme activity in muscle fibers. Journal of Histochemistry & Cytochemistry 1998;46(2):275–276.

[46] Steinberg, D.K., Van Mooy, B.A., Buesseler, K.O., Boyd, P.W., Kobari, T., Karl, D.M.. Bacterial vs. zooplankton control of sinking particle flux in the ocean's twilight zone. Limnology and Oceanography 2008;53(4):1327–1338.

[47] Suelter, C.H., et al. Practical guide to enzymology. Wiley, 1985.

[48] Tames-Espinosa, M., Martinez, I., Romero-Kutzner, V., Bondyale-Juez, D., Packard, T., Gomez, M., Under-Submission, X.. Potential CO_2 production from $NADP^+$-dependent isocitrate dehydrogenase in marine planktonic organisms. Progress in Oceanography 2018;000:000–000.

[49] Walsh, K., Koshland, D.E.. Determination of flux through the branch point of two metabolic cycles. The tricarboxylic acid cycle and the glyoxylate shunt. Journal of Biological Chemistry 1984;259(15):9646–9654.

[50] Whitaker, J.R.. Principles of enzymology for the food sciences. volume 61. CRC Press, 1993.

[51] Wieckowski, M.R., Giorgi, C., Lebiedzinska, M., Duszynski, J., Pinton, P.. Isolation of mitochondria-associated membranes and mitochondria from animal tissues and cells. Nature protocols 2009;4(11):1582.

[52] Williamson, J.R., Cooper, R.H.. Regulation of the citric acid cycle in mammalian systems. FEBS letters 1980;117(S1):K73–K85.

7. Appendix A. Supplementary information: Extended information

7.1. Buffer studies

An enzymatic assay is performed on buffered reaction mixtures containing cofactors and effectors. Here, the optimum combination between buffer and the main cationic effectors (Mg^{2+} or Mn^{2+}) was obtained from ten different experiments that were run at 18°C, pH 8.5, 4mM isocitrate, 0.08mM $NADP^+$ and 2mM $MgCl_2$ on five different concentrations of purified NADP-IDH from porcine heart (I2002, Sigma Aldrich) (zooplankton samples were not used here in order to maintain the same sample conditions in every experiment). Preliminary tests were performed to determine the range of purified NADP-IDH concentrations needed to optimize this study. The response in the enzyme activity was analysed for different combinations of buffer, cationic effector (Kornberg and Pricer [18], Munilla-Moran and Stark [25]) and the presence of lysozyme in the homogenisation buffer (Berdalet et al. [5]): (1) 25mM MOPS, 2mM $MgCl_2$ and 0.167mg mL^{-1} lysozyme (SIGMA L6876); (2) 25mM MOPS and 2mM $MgCl_2$; (3) 25mM MOPS, 2mM $MnCl_2{\cdot}4H_2O$ (PANREAC 131410) and 0.167mg mL^{-1} lysozyme; (4) 25mM MOPS and 2mM $MnCl_2{\cdot}4H_2O$; (5) 0.1M phosphate buffer, 2mM $MgCl_2$ and 0.167mg mL^{-1} lysozyme; (6) 0.1M phosphate buffer and 2mM $MgCl_2$; (7) 0.1M TRIS 2mM $MgCl_2$ and 0.167mg mL^{-1} lysozyme; (8) 0.1M TRIS and 2mM $MgCl_2$; (9) 0.1M TRIS, 2mM $MnCl_2{\cdot}4H_2O$ and 0.167mg mL^{-1} lysozyme; (10) 0.1M TRIS and 2mM $MnCl_2{\cdot}4H_2O$. Results were based on triplicate measurements. NADP-IDH activity was reported in μmol NADPH min^{-1}(mL of homogenate)$^{-1}$ units.

NADP-IDH activity in phosphate buffer resulted to be 45.88% higher than the next higher activity (in MOPS) for the same dilute enzyme solution in the lowest concentration (the closest to zooplankton samples, 1 μmol NADPH min^{-1} mL^{-1} in the X axis of Fig.7). No results for Mn^{2+}-phosphate buffer were obtained because Mn^{2+} reacted with the phosphate to give a $Mn_3(PO_4)_2$ precipitate, resulting in a competing chemical reaction among the reagents that prevented correct readings of the spectrophotometer. Given the reactivity of Mn^{2+} with phosphate buffer, Mn^{2+} was eliminated and Mg^{2+} was selected as the metal cation for this assay.

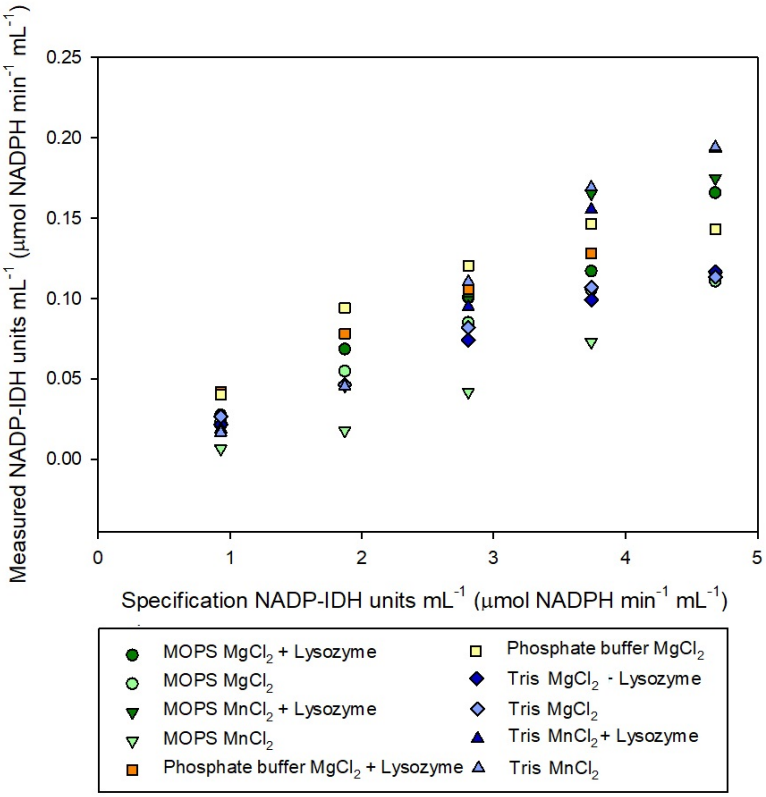

Figure 7: Buffer effects on NADP-IDH activity

7.2. Molar extinction coefficient (ϵ) studies

This assay is based on spectrophotometry, the Beer-Lambert law, and the absorbance at 340nm (A_{340}), all of which go to determine the concentration of NADPH (Section 2.2). To accomplish this we needed to determine the molar extinction coefficient (ϵ) for the NADPH in our specific reactant solution. The molar extinction coefficient (ε) is a measurement of the attenuation of light, at a specific wavelength, due to a molar concentration of the target chemical species. It quantifies the relationship between the light absorbance and the concentration of the chemical species. Thus, ϵ for the NADPH was analysed at pH 8.5 and 18°C by measuring absorbance at 340nm (A_{340}) under simu-

lated reaction conditions and simulated blank conditions. Ten different concentrations of NADPH, ranging from 0.08 to 40μM, were prepared with three solutions (Supplementary information: Tables 15, 16 and 17): (1) phosphate buffer 0.1M, 2mM isocitrate and 3.3mM $MgCl_2$; (2) phosphate buffer 0.1M and 3.3mM $MgCl_2$; and (3) only phosphate buffer 0.1M. Results were based on triplicate measurements. The molar extinction coefficient was reported in absortivity units mL μmol^{-1} cm^{-1}.

Reported NADPH ε in the literature is 6.2 L mmol^{-1} cm^{-1} (Morris and Redfearn [23]), which was measured at pH 7.5 in a solution different from the buffer in our NADP-IDH assay. In our hands, Fig.8, the increase of absorbance per mmol L^{-1} of NADPH was similar for the three experiments (5.21 L mmol^{-1} cm^{-1} for the phosphate buffer, 5.35 L mmol^{-1} cm^{-1} for the phosphate buffer with $MgCl_2$ and 5.42 L mmol^{-1}cm^{-1}, for the phosphate buffer with $MgCl_2$ and isocitrate). Our reaction solution is similar to the third buffer, so we will use an ε of 5.42L mmol^{-1} cm^{-1} in our calculations. If we were to use an ε from the literature (6.2 L mmol^{-1} cm^{-1}) we would introduce an error of 12.6%.

Note that the ε increased with the complexity of the buffer solution. So, testing the ε related to product measurements on the solution where reaction is happening, would be a good practice to reduce error in future measurements.

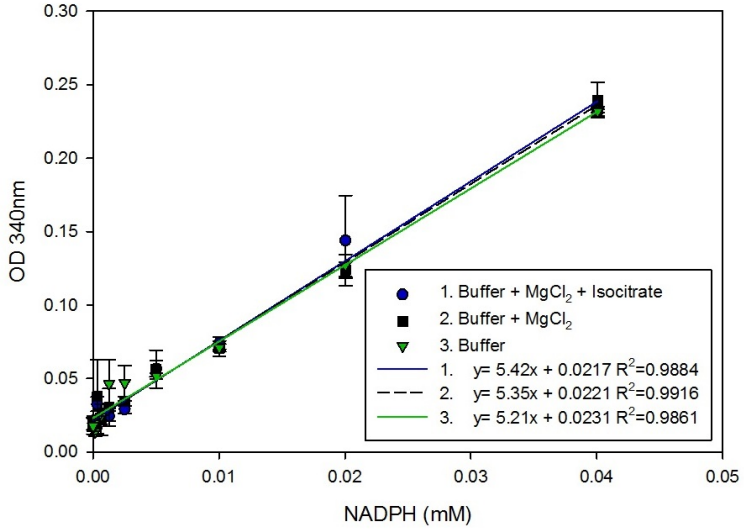

Figure 8: NADPH molar extinction coefficient, in three different buffer combinations (Supplementary information: Tables 15, 16, and 17).

7.3. Kinetics

The NADP-IDH activity related to the substrate concentration showed a rectangular hyperbolic relationship for isocitrate and $NADP^+$, following the expression represented in Eq.11.

$$\%V_{max}=a\cdot[S]/(y_0+[S]) \quad (11)$$

The values of "a", which represents the V_{max} (in this case, the % of V_{max}) and "y_0", which represents the K_m are shown in Table 2. NADP-IDH dependences on isocitrate were not significantly different among these samples (F test, $F_{(4,63)}$=1.73, p=0.01). On the other hand, dependence on $NADP^+$ showed significant differences among the three size-fractions (F test, $F_{(4,69)}$=6.85, p=0.01). Even though the regressions were different, the average K_m and optimum values in both experiments can be properly used in our assay in order to obtain the V_{max} for the whole plankton community. Furthermore, although they are significant differences in the NADP-IDH and $MgCl_2$ affinity among the samples (F test, $F_{(4,114)}$=2.75, p=0.01), the optimal value obtained by inspection of Fig.2, can be properly used for our assay in order to obtain the V_{max} for the whole plankton community (6mM $MgCL_2$ for the whole community).

We applied three main linearisation techniques to accurately evaluate the K_ms of isocitrate and $NADP^+$. In the Hanes-Woolf linearisation, substrate concentration [S] was plotted against concentration per enzymatic activity ([S]/V). The V_{max} was obtained from the inverse of the slope (a) ($V_{max} = 1/a$), whereas K_ms were equal to the ratio of the Y intercept (y_0) and a ($K_m = y_0/a$) (Suelter et al. [47]). In the case of the Lineweaver-Burk method, the inverse of the substrate (1/[S]) was plotted against the inverse of the activity (1/V), so the V_{max} was the inverse of y_0 (V_{max}=$1/y_0$) and $K_m = a/y_0$. Finally, using the Eadie-Hofstee methodology we plotted V/[S] against V, where the $V_{max} = y_0$ and K_m =-y_0/a. K_m was reported in mmol of substrate, and V_{max} in μmol NADPH min^{-1}(mL of homogenate)$^{-1}$ units (Suelter et al. [47]).

Finally, Hanes-Woolf linearisation was the most accurate to our data base for both isocitrate and NADP $^+$ (p<0.001) (Supplementary information, Table 10). The apparent Kms of 271$\pm$63μM of isocitrate and 18$\pm$3μM of $NADP^+$ are consistent with those obtained by the

Michaelis-Menten hyperbolic regressions.

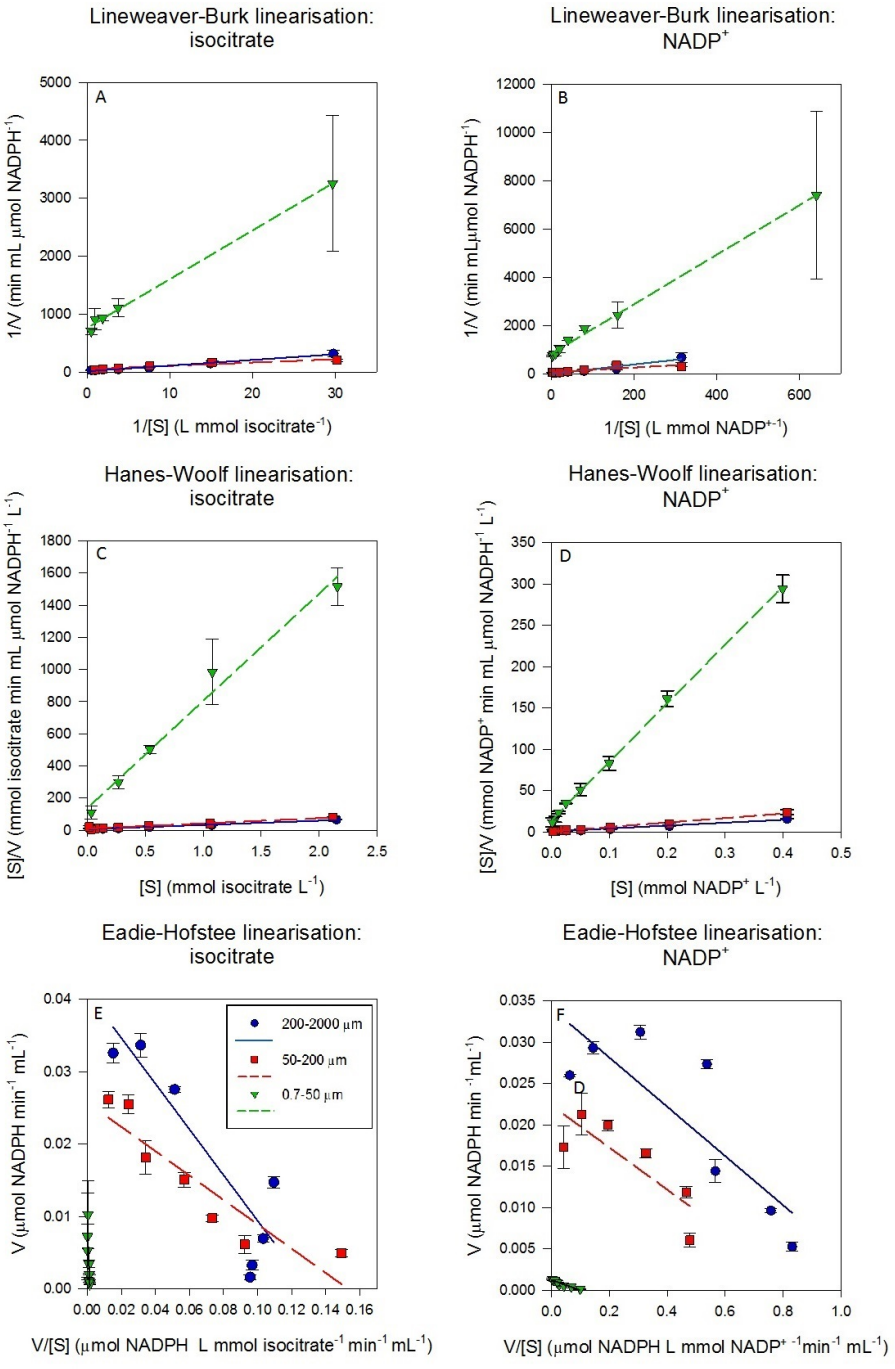

Figure 9: Hanes-Woolf, Lineweaver-Burk and Eadie-Hofstee linearisations to determine the affinity (K_m) of NADP-IDH for $NADP^+$ and isocitrate in marine-plankton samples (Supplementary information: Table 10). The symbols in the key of panel E apply to all six panels.

7.4. pH effects

Michaelis-Menten constants are affected by pH levels that impact ionisation around the enzyme active site. Thus, the conformations of the active site, the binding of substrate to the enzyme, and/or the transformation from substrates to products may be altered. This ionisation is sensitive to the chemical solution, shifting the pK_a values in relation to the nature of the buffer solution (Whitaker [50]). Although we have not checked the K_ms for every pH condition, during the pH experiments we maintained concentrations of isocitrate and $NADP^+$ high enough to broadly saturate the enzyme at pH 8.5, assuming the V_{max} was reached at every experimental pH level. Finally, a pH of 8.2 (Fig.10) resulted to be the marine NADP-IDH optimum, with p$K-a$s at 7.62 and 8.75. For Fig.10, results were normalised by V_{max} and reported as a percentage.

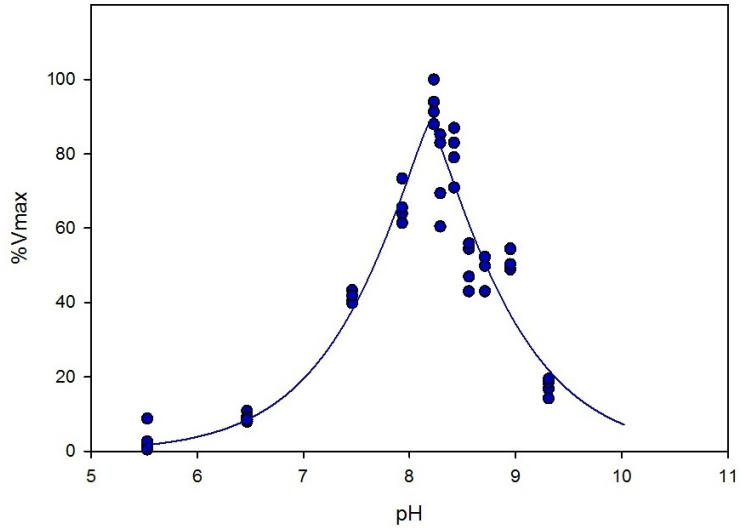

Figure 10: pH effects on NADP-IDH activity (Supplementary information: Tables 11 and 12).

7.5. Temperature effects: Development of the Arrhenius equation

Another reason for determining the Arrhenius relationship between NADP-IDH activity and T, is to correct measurements when environ-

mental T is different from the measurement T. If plankton samples were assayed at the in-situ T from a low temperature environment, there is a risk that the NADP-IDH signal would fall below the limit of detection. Accordingly, enzyme activities are measured at T above the in-situ one (Packard [31]) and converted back to the activity at in-situ T using the Arrhenius equation (Fig.3) (Packard [31]). This equation is equivalent to Van't Hoff equation (Atkin and de Paula [4]), as expressed on Eq.12, 13 and 14:

$$\ln(K_2/K_1) = (Ea/R)\cdot((1/T_1)\text{-}(1/T_2)) \quad (12)$$

Taking anti-logarithms we obtained the ratio of the rate constants:

$$K_2/K_1 = \exp((Ea/R)\cdot((1/T_1)\text{-}(1/T_2))) \quad (13)$$

Then, we transposed to solve for the in-situ rate:

$$K_2 = K_1 \cdot exp((Ea/R) \cdot ((1/T_1)\text{-}(1/T_2))) \quad (14)$$

where: K_2 is the in-situ reaction rate and K_1 is the measured reaction rate at T_2 (in-situ T) and T_1 (measurement T) respectively, in μmol NADPH min^{-1} mL^{-1}; Ea is the energy of activation in Kcal mol^{-1}; R is the molar gas constant in Kcal mol^{-1} $^oK^{-1}$; and T_1 and T_2 are temperatures in ^{o}K.

In the case of the marine plankton NADP-IDH, with an Ea of 20.39 Kcal mol^{-1} NADP-IDH activity for the in-situ T (T_i) is obtained by applying Eq.15:

$$\text{NADP-IDH}(T_i) = \text{NADP-IDH}(T_m) \cdot exp((20.39/R) \cdot (1/T_m\text{-}1/T_i)) \quad (15)$$

where: NADP-IDH(T_i) is NADP-IDH activity at in-situ temperature; NADP-IDH(T_m) is NADP-IDH activity at temperature in the spectrophotometric cuvette during measurement; R is $1.9872 \cdot 10^{-3}$ Kcal mol^{-1} $^oK^{-1}$; T_m is temperature in the spectrophotometric cuvette during measurement in ^{o}K; and T_i in-situ temperature in ^{o}K.

7.6. Precision studies

The precision of this assay was tested on four different solutions of porcine heart NADP-IDH (I2002, Sigma Aldrich). These solutions where made by diluting the original solution (93.6units of NADP-IDH mL^{-1}), resulting in four solutions which ranged from 0.0004 to 0.25 units of NADP-IDH mL^{-1} which were reported in specification units (*UsIDH*, *i.e.*, μmol NADPH min^{-1} (mL of homogenate)$^{-1}$). Ten duplicates were used for every solution. Note that one unit (U) of enzyme activity was defined as the amount of sample able to catalyse the production of 1μmol NADPH in 1 min.

Precision was scaled by using the standard deviation with the optimum pH and ligands from previous experiments (pH 8.2, 6mM $MgCl_2$, 2.1mM isocitrate and 0.2mM $NADP^+$). The measurement was made at 37.5°C for comparison with the theoretical characteristics of pure porcine heart NADP-IDH (specification sheet I2002 by Sigma Aldrich). Results were tested in ten samples for every solution and reported as measured units (*UmIDH*), in μmol NADPH min^{-1} (mL of homogenate)$^{-1}$.

The average standard deviation was 1.2nmol NADPH min^{-1}, ranging from 0.6nmol in the two lower values, to 2nmol NADPH min^{-1} in the most concentrated ones (Fig.11). On a percentage basis, except for the lowest value, where it represented 25% of the sample value, the standard deviation was less than 3.5% for the samples with more than 25nmol NADPH min^{-1}, dropping to 1.73% for the highest concentration (Fig.11).

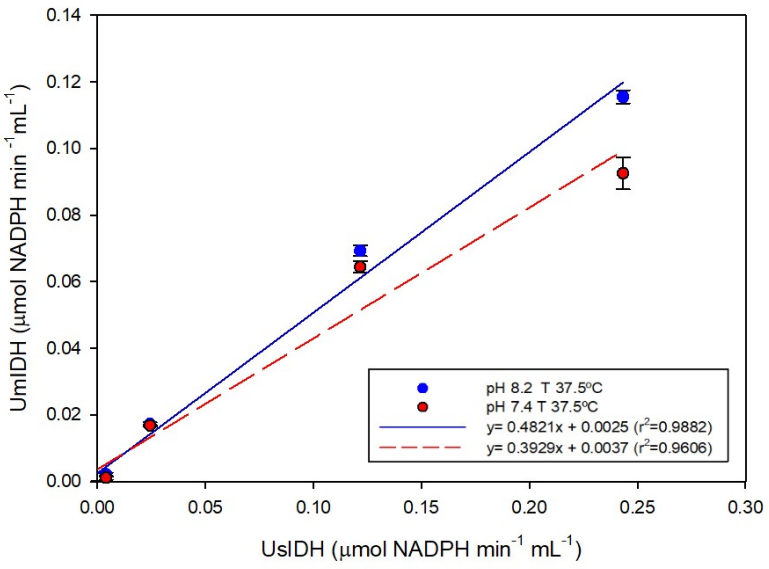

Figure 11: Porcine-heart NADP-IDH activity measured by the marine-plankton NADP-IDH assay at pH:8.2 and pH:7.4 (Supplementary information: Tables 18 and 19)

Using our new NADP-IDH assay we also measured the activity of the Sigma-Aldrich porcine-heart NADP-IDH. We used the same pH and T as those specified in the Sigma-Aldrich specification sheet (pH=7.4; T=37.5ºC), and found 39.3% of the theoretical activity (Fig.11, Supplementary information: Table 19). When we measured the activity at pH 8.2 (optimum value in Fig.10) we found 48.2% (Fig.11) of the theoretical activity. The use of pure-porcine NADP-IDH activity to normalise the method is useful to compare with other samples, organisms and methodologies. In our hands, one unit (μmol NADPH min^{-1}) of NADP-IDH activity in marine plankton homogenates, was equivalent to 2.08 pure porcine-heart NADP-IDH units, by applying the equation obtained from Fig.11 and Eq.16. This equation pertains to the optimum conditions of our new NADP-IDH method:

$$UmIDH = 0.48 \cdot UsIDH + 0.0029 \quad (16)$$

where *UmIDH* refers to NADP-IDH activity units as measured by the new method, and *UsIDH* refers to the specification NADP-IDH activity

units as calculated for the pure porcine-heart NADP-IDH solutions.

In the linear range of Fig.11, which describes the increase in NADP-IDH activity as a function of enzyme concentration, it is clear that the substrate concentrations are sufficient to maintain maximum activity until 0.25 *UsIDH* units of NADP-IDH (which represents a measured value of 0.12UmIDH with our methodology). Samples from the Canary Islands plankton never reached such a high value (Section 3.4, Supplementary information Table 20), so they were always in the linear range. For future plankton samples, if a pilot test were to show activity above 0.12 *UmIDH* μmol NADPH $\text{min}^{-1}\text{mL}^{-1}$, the homogenate would need dilution.

7.7. Understanding changes in the NADP-IDH spectrophotometrical response

A linear A_{340} increasing (Fig.12(A)) is expected when NADP-IDH is catalysing the reaction at V_{max}. However, in marine plankton samples, some conditions may change this linearity as follows:

1 Low Biomass samples (Fig.12(B)). Under these conditions, the rate of NADPH formation is low, and the signal was not detectable for the first 500s. The NADP-IDH activity, in this case, is under the limit of detection. If more biomass is not available, sensitivity can be obtained by raising the reaction temperature to 30°C and applying the Arrhenius equation to correct the activity to that of the in-situ T (Eq. 17).

2 T effects (Fig.12(C)). Depending on the difference between the laboratory T and the spectrophotometer read-out T, the reaction temperature will lag until thermal equilibrium is reached in the cuvette. We monitored T in the cuvette over time and for 8 to 46°C range, and found that steady-state was reached after 450s. We suggest that enzyme activity measurements should be made only after this lag-period (7.5 min). If the plateau zone is reached within the first 500s, the cuvette might not have reached the equilibrium T. In this case, we suggest repeating the measurement with a diluted sample. Given the importance of T and all the problems with maintaining it in the cuvette, we also suggest measuring T in the cuvette at the end of the reaction.

3 High Biomass samples (Fig.12(D)). The optimum values for NADP-IDH substrates reported on this study have proved to work well for the biomass levels found in plankton samples around the Canary Islands archipelago. Eventually, the reagents are completely consumed when the A_{340} reaches 0.8. After that point, the reaction becomes non-linear, underestimating the V_{max}.

4 Blank effects (Fig.12(E)). Working with natural homogenates, instead of pure enzyme extracts, rises interference from other enzymes oxidizing the produced NADPH. Although this effect is not usually significant because these enzymes are not supplied with their other substrates, eventually, some samples will produce negative blanks that could significantly increase the results. Particle sinking in the cuvette due to low centrifugation may also affect the measurements in this way (Section 3.5). To minimise the sedimentation effect we recommend centrifugation (at least 2 min at 1000rpm for 50-2000μm samples, or 10min at 4000rpm for 0.7-50μm samples collected on 0.7GF/F filters). If the condition persists, even after the centrifugation, and the blank remains negative, a background reaction is likely real and has to be taken into account.

During the T and pH experiments, great differences in the slopes (the velocity of the reaction) at different levels of T or pH were observed (Fig. 13) Higher slopes were observed near the optimum values. Temperatures shown in Fig. 13 represent final T in the cuvette. When this temperature was close to the temperature of the lab (around 21°C), we obtained the same slope for 1500s, throughout the measurement. However, when the reaction temperatures were far from the laboratory T, time was needed for the cuvette to reach thermal equilibrium. As said before, we have observed that 500s ensures a good measurement at the selected temperature. Furthermore, when T higher than 30°C is used, denaturation of the enzyme becomes a factor that needs to be considered (Fig.13(a)).

Thus, cuvette temperature should be measured before the assay is initiated, to make sure that the target temperature has been reached after the cuvette has been placed into the thermostatted cell holder of the spectrophotometer.

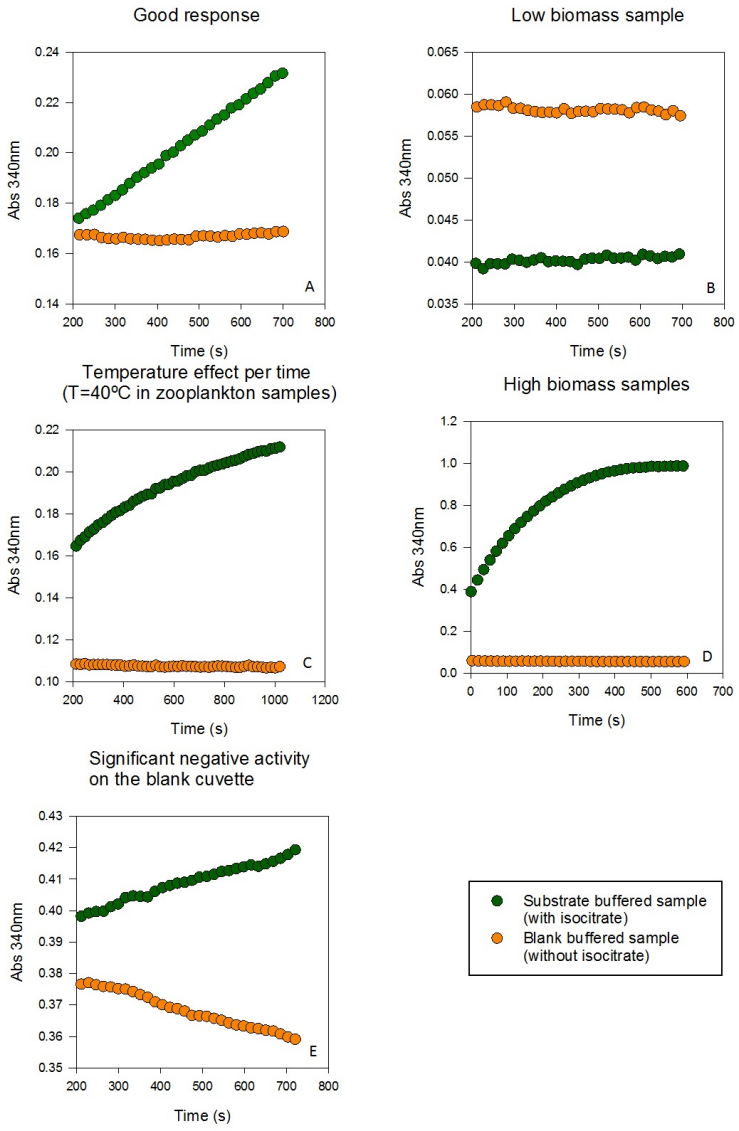

Figure 12: Spectrophotometrical response of NADP-IDH activity, following the A_{340} per time of the substrate and blank buffered cuvettes, under conditions that affect the signal during the measurement

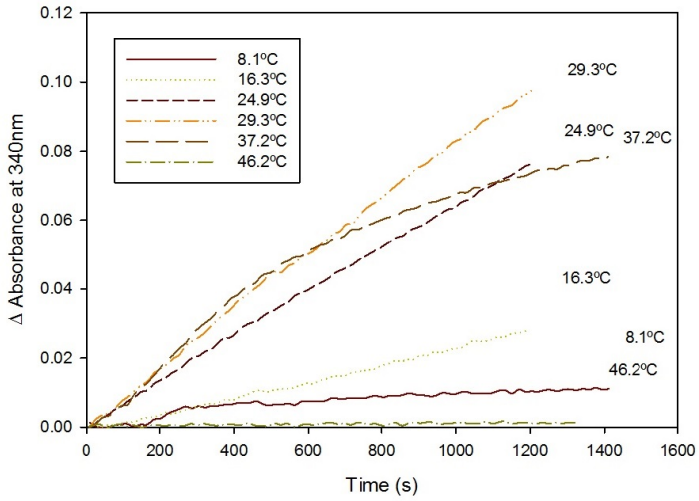

(a) Temperature effects on NADP-IDH activity by the kinetic assay.

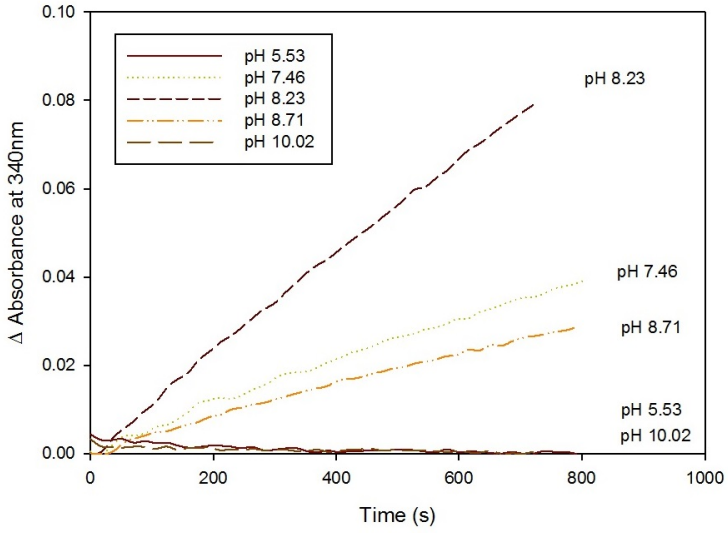

(b) pH effects on NADP-IDH activity by the kinetic assay.

Figure 13: Kinetic responses of NADP-IDH to different levels of T and pH.

8. Appendix B. Supplementary information: Tables

Table 1: Experimental database to analyse the NADP-IDH affinity with isocitrate, in the 200-2000μm size-fractionated community

Sample	Isocitrate mM	NADP-IDH μmol min^{-1} mL^{-1}	%V$_{max}$	Average	SD	Hyperbola curve a (%V$_{max}$)	b (K_m)	r^2	*p-value*
200-2000μm	2.150	0.033681	95.86						
	2.150	0.031024	88.30	92.67	3.92				
	2.150	0.032983	93.87						
	1.075	0.031849	90.64						
	1.075	0.035137	100.00	95.74	4.73				
	1.075	0.033930	96.57						
	0.538	0.027199	77.41						
	0.538	0.027404	77.99	78.29	1.06				
	0.538	0.027924	79.47						
	0.269	0.021717	61.81						
	0.269	0.022716	64.65	63.64	1.59				
	0.269	0.022649	64.46						
	0.134	0.014253	40.56						
	0.134	0.014220	40.47	41.87	2.35	109.34	0.225	0.99	<0.0001
	0.134	0.015664	44.58						
	0.067	0.006554	18.65						
	0.067	0.007461	21.24	19.75	1.33				
	0.067	0.006803	19.36						
	0.034	0.002828	8.05						
	0.034	0.004046	11.52	9.25	1.96				
	0.034	0.002878	8.19						
	0.017	0.001317	3.75						
	0.017	0.001550	4.41	4.57	0.91				
	0.017	0.001948	5.55						
	0.008	0.001876	5.34						
	0.008			4.33	1.43				
	0.008	0.001168	3.32						

Table 2: Experimental database to analyse the NADP-IDH affinity with isocitrate, in the 50-200μm size-fractionated community

Sample	Isocitrate mM	NADP-IDH μmol min^{-1} mL^{-1}	%V$_{max}$	Average	SD	Hyperbola curve a (%V$_{max}$)	b (K_m)	r^2	*p-value*
50-200μm	2.120	0.027387	100.00	95.39	4.26	109.25	0.269	0.98	<0.0001
	2.120	0.025085	91.59						
	2.120	0.025899	94.56						
	1.060	0.026507	96.79	93.07	4.62				
	1.060	0.024072	87.89						
	1.060	0.025887	94.52						
	0.530	0.015426	56.33	66.07	8.45				
	0.530	0.019517	71.26						
	0.530	0.019345	70.63						
	0.265	0.014214	51.90	54.96	3.74				
	0.265	0.014751	53.86						
	0.265	0.016196	59.14						
	0.133	0.009238	33.73	35.53	1.69				
	0.133	0.010157	37.09						
	0.133	0.009797	35.77						
	0.066	0.005225	19.08	22.35	4.50				
	0.066	0.007528	27.49						
	0.066	0.005613	20.49						
	0.033	0.005419	19.79	18.04	1.80				
	0.033	0.004434	16.19						
	0.033	0.004970	18.15						
	0.017			2.86	0.70				
	0.017	0.000648	2.36						
	0.017	0.000919	3.35						

Table 3: Experimental database to analyse the NADP-IDH affinity with isocitrate, in the 0.7-50μm size-fractionated community

Sample	**Isocitrate** mM	**NADP-IDH** μmol min^{-1} mL^{-1}	%V$_{max}$	**Average**	**SD**	**Hyperbola curve** a (%V$_{max}$)	b (K_m)	r^2	***p-value***
	2.159	0.001517	100.00						
	2.159	0.001312	86.50	94.28	6.99				
	2.159	0.001461	96.35						
	1.079	0.001218	80.29						
	1.079	0.000886	58.39	74.21	13.82				
	1.079	0.001273	83.94						
	0.540	0.001052	69.34						
	0.540	0.001135	74.82	70.80	3.52				
	0.540	0.001035	68.25						
	0.270	0.001068	70.44						
	0.270	0.000803	52.92	60.46	9.01				
	0.270	0.000880	58.03						
	0.135	0.000304	20.07						
0-7-50μm	0.135	0.000387	25.55	28.35	9.97	96.99	0.203	0.96	<0.0001
	0.135	0.000598	39.42						
	0.067	0.000399	26.28						
	0.067	0.000459	30.29	28.28	2.84				
	0.067								
	0.034	0.000249	16.42						
	0.034	0.000260	17.15	22.75	10.33				
	0.034	0.000526	34.67						
	0.017								
	0.017	0.000133	8.76	5.84	4.13				
	0.017	0.000044	2.92						
	0.008	0.000072	4.74						
	0.008	0.000105	6.93	4.01	3.34				
	0.008	0.000006	0.36						

Table 4: Experimental database to analyse the NADP-IDH affinity with $NADP^+$, in the 200-2000μm size-fractionated community

Sample	$NADP^+$ mM	NADP-IDH μmol min^{-1} mL^{-1}	$\%V_{max}$	Average	SD	Hyperbola curve a ($\%V_{max}$)	b (K_m)	r^2	*p-value*
	0.4070	0.026170	82.23						
	0.4070	0.025838	81.18	81.63	0.54				
	0.4070	0.025937	81.50						
	0.2035	0.030127	94.66						
	0.2035	0.028638	89.98	92.07	2.38				
	0.2035	0.029142	91.57						
	0.1018	0.031544	99.11						
	0.1018	0.030288	95.17	98.09	2.57				
	0.1018	0.031827	100.00						
	0.0509	0.027382	86.03						
	0.0509	0.026835	84.31	85.94	1.58				
	0.0509	0.027841	87.48						
	0.0254	0.014137	44.42						
200-2000μm	0.0254	0.015886	49.91	45.29	4.26	102.75	0.024	0.9255	<0.0001
	0.0254	0.013218	41.53						
	0.0127	0.009836	30.90						
	0.0127			30.30	0.85				
	0.0127	0.009454	29.70						
	0.0064	0.005662	17.79						
	0.0064			16.62	1.66				
	0.0064	0.004915	15.44						
	0.0032	0.001196	3.76						
	0.0032	0.002275	7.15	5.10	1.80				
	0.0032	0.001395	4.38						
	0.0004								
	0.0004	0.001600	5.03	5.03					
	0.0004								

Table 5: Experimental database to analyse the NADP-IDH affinity with $NADP^+$, in the 50-200μm size-fractionated community

Sample	$NADP^+$ mM	NADP-IDH μmol min^{-1} mL^{-1}	$\%V_{max}$	Average	SD	Hyperbola curve a ($\%V_{max}$)	b (K_m)	r^2	*p-value*
	0.4070	0.020197	86.12						
	0.4070	0.015244	65.00	73.95	10.92				
	0.4070	0.016589	70.73						
	0.2035	0.023452	100.00						
	0.2035	0.021869	93.25	90.74	10.74				
	0.2035	0.018520	78.97						
	0.1018	0.020574	87.73						
	0.1018	0.019821	84.52	84.99	2.53				
	0.1018	0.019400	82.72						
	0.0509	0.017175	73.24						
	0.0509	0.016522	70.45	70.73	2.38				
	0.0509	0.016063	68.49						
50-200μm	0.0254	0.011779	50.22			93.45	0.023	0.9296	0.0001
	0.0254	0.011170	47.63	50.55	3.09				
	0.0254	0.012614	53.79						
	0.0127	0.006825	29.10						
	0.0127	0.005164	22.02	25.93	3.60				
	0.0127	0.006255	26.67						
	0.0064	0.003421	14.59						
	0.0064			12.77	2.56				
	0.0064	0.002571	10.96						
	0.0032	0.003343	14.26						
	0.0032	0.003482	14.85	14.55	0.42				
	0.0032								

Table 6: Experimental database to analyse the NADP-IDH affinity with $NADP^+$, in the 0.7-50μm size-fractionated community

Sample	$NADP^+$ mM	NADP-IDH μmol min^{-1} mL^{-1}	$\%V_{max}$	Average	SD	Hyperbola curve a ($\%V_{max}$)	b (K_m)	r^2	*p-value*
0.7-50μm	0.3994	0.001450	100.00						
	0.3994	0.001334	91.98	93.89	5.41				
	0.3994	0.001301	89.69						
	0.1997	0.001301	89.69						
	0.1997	0.001162	80.15	85.75	4.98				
	0.1997	0.001268	87.40						
	0.0999	0.001334	91.98						
	0.0999	0.001085	74.81	83.59	8.59				
	0.0999	0.001218	83.97						
	0.0499	0.000869	59.92						
	0.0499	0.001162	80.15	68.32	10.54				
	0.0499	0.000941	64.89						
	0.0250	0.000581	40.08			96.83	0.020	0.9807	<0.0001
	0.0250	0.000725	50.00	46.56	5.62				
	0.0250	0.000720	49.62						
	0.0125	0.000504	34.73						
	0.0125	0.000542	37.40	36.90	1.96				
	0.0125	0.000559	38.55						
	0.0062	0.000410	28.24						
	0.0062	0.000338	23.28	29.52	6.96				
	0.0062	0.000537	37.02						
	0.0016	0.000216	14.89						
	0.0016	0.000089	6.11	10.69	4.40				
	0.0016	0.000161	11.07						

Table 7: Experimental database to analyse the NADP-IDH affinity with $MgCl_2$, in the 200-2000μm size-fractionated community

Sample	**$MgCl_2$ mM**	**NADP-IDH μmol min^{-1} mL^{-1}**	**%V$_{max}$**	**Average**	**SD**	**Sigmoid curve**				
						a	**b**	**X$_0$**	**r^2**	***p-value***
	5.990	0.007085	100.00							
	5.990	0.006946	98.05	99.02	1.38					
	5.990									
	2.995	0.006293	88.83							
	2.995	0.006244	88.13	91.85	5.85					
	2.995	0.006985	98.59							
	1.497	0.004118	58.13							
	1.497	0.004749	67.03	61.56	4.79					
	1.497	0.004218	59.53							
	0.748	0.002386	33.67							
200-2000μm	0.748	0.001799	25.39	27.29	5.67	97.08	0.514	1.221	0.9961	<0.0001
	0.748	0.001616	22.81							
	0.374	0.001478	20.86							
	0.374	0.001162	16.41	19.51	2.69					
	0.374	0.001506	21.25							
	0.187	0.000792	11.17							
	0.187	0.000576	8.13	9.30	1.64					
	0.187	0.000609	8.59							
	0.094	0.000692	9.77							
	0.094			7.07	3.81					
	0.094	0.000310	4.38							

Table 8: Experimental database to analyse the NADP-IDH affinity with $MgCl_2$, in the 50-200μm size-fractionated community

Sample	**$MgCl_2$ mM**	**NADP-IDH μmol min^{-1} mL^{-1}**	**%V$_{max}$**	**Average**	**SD**	**Sigmoid curve**				
						a	**b**	**X$_0$**	**r^2**	***p-value***
50-200μm	5.990	0.004423	79.27							
	5.990	0.005469	98.02	92.43	11.44					
	5.990	0.005579	100.00							
	2.995	0.004710	84.42							
	2.995	0.004389	78.67	85.48	7.40					
	2.995	0.005208	93.35							
	1.497	0.002469	44.25							
	1.497	0.003493	62.60	57.14	11.21					
	1.497	0.003603	64.58							
	0.748	0.001771	31.75			90.20	0.504	1.199	0.9928	0.0006
	0.748	0.001306	23.41	29.99	5.90					
	0.748	0.001943	34.82							
	0.374	0.000808	14.48							
	0.374	0.000764	13.69	14.42	0.70					
	0.374	0.000841	15.08							
	0.187	0.000426	7.64							
	0.187	0.000238	4.27	5.95	2.39					
	0.187									

Table 9: Experimental database to analyse the NADP-IDH affinity with $MgCl_2$, in the 0.7-50μm size-fractionated community

Sample	**$MgCl_2$ mM**	**NADP-IDH μmol min^{-1} mL^{-1}**	**%V_{max}**	**Average**	**SD**	**Sigmoid curve**				
						a	**b**	**X_0**	**r^2**	***p-value***
0.7-50μm	10.440	0.000603	45.42							
	10.440	0.001323	99.58	71.94	27.10					
	10.440	0.000941	70.83							
	7.830	0.001173	88.33							
	7.830	0.001245	93.75	90.69	2.77					
	7.830	0.001196	90.00							
	5.220	0.000985	74.17							
	5.220	0.001328	100.00	80.56	17.17					
	5.220	0.000897	67.50							
	2.610	0.000625	47.08							
	2.610	0.000603	45.42	47.64	2.55					
	2.610	0.000670	50.42							
	1.305	0.000432	32.50			82.45	1.159	2.047	0.9662	0.0002
	1.305	0.000376	28.33	29.86	2.29					
	1.305	0.000382	28.75							
	0.653	0.000327	24.58							
	0.653	0.000310	23.33	22.64	2.37					
	0.653	0.000266	20.00							
	0.326	0.000188	14.17							
	0.326	0.000210	15.83	15.42	1.10					
	0.326	0.000216	16.25							
	0.163	0.000221	16.67							
	0.163	0.000138	10.42	10.56	6.04					
	0.163	0.000061	4.58							

Table 10: Experimental database to analyse the apparent isocitrate and NADP$^+$ K_m values calculated by Hanes-Woolf, Lineweaver-Burk and Eadie-Hofstee linearisations

		Linear regression Hanes-Woolf				**Hanes-Woolf results**	
		a (slope)	**y_0**	**r^2**	***p-value***	***K_m* (y_0/a)**	**V_{max} (1/a)**
Isocitrate	**200-2000μm**	26.29	7.16	0.9835	<0.0001	0.273	0.03804
	50-200μm	32.41	10.83	0.9605	<0.0001	0.334	0.03085
	0.7-50μm	666.41	138.32	0.9823	0.001	0.208	0.00150
NADP$^+$	**200-2000μm**	34.84	0.74	0.974	<0.0001	0.021	0.02870
	50-200μm	53.57	0.73	0.9772	<0.0001	0.014	0.01867
	0.7-50μm	708.16	13.91	0.9988	<0.0001	0.020	0.00141
		Linear regression Lineweaver-Burk				**Lineweaver-Burk results**	
		a (slope)	**y_0**	**r^2**	***p-value***	***K_m* (a/y_0)**	**V_{max} (1/y_0)**
Isocitrate	**200-2000μm**	9.79	13.15	0.986	<0.0001	0.745	0.07605
	50-200μm	5.67	49.84	0.921	0.0024	0.114	0.02007
	0.7-50μm	84.07	765.98	0.9964	<0.0001	0.110	0.00131
NADP$^+$	**200-2000μm**	1.93	-4.66	0.9382	<0.0001	-0.413	-0.21467
	50-200μm	0.94	63.93	0.7565	0.005	0.015	0.01564
	0.7-50μm	10.26	827.28	0.9971	<0.0001	0.012	0.00121
		Linear regression Eadie-Hoffstee				**Eadie-Hofstee results**	
		a (slope)	**y_0**	**r^2**	***p-value***	***K_m* (-y_0/a)**	**V_{max} (y_0)**
Isocitrate	**200-2000μm**	-0.32	0.04	0.7532	0.0052	0.130	0.04090
	50-200μm	-0.17	0.03	0.8366	0.0039	0.153	0.02570
	0.7-50μm	-5.34	0.01	0.691	0.0205	0.002	0.00810
NADP$^+$	**200-2000μm**	-0.03	0.03	0.7077	0.0177	1.148	0.03410
	50-200μm	-0.03	0.02	0.6893	0.0408	0.878	0.02240
	0.7-50μm	-0.01	0.00	0.8882	0.0005	0.106	0.00130

Table 11: Experimental database to analyse the pH effects in 200-2000μm size-fractioned NADP-IDH activity (1/2)

pH	**NADP-IDH** (μmol NADPH $min^{-1}mL^{-1}$)	**mg protein** mL^{-1}	**NADP-IDH** (μmol NADPH min^{-1}mg $protein^{-1}$)	$\%V_{max}$	**Average**	**SD**
10.02	-0.00012	0.21	-0.00059	-2.22		
10.02	0.00000	0.20	-0.00001	-0.05	-2.26	1.76
10.02	-0.00013	0.20	-0.00064	-2.40		
10.02	-0.00025	0.21	-0.00116	-4.36		
9.31	0.00123	0.27	0.00449	16.83		
9.31	0.00133	0.27	0.00494	18.50	17.25	2.29
9.31	0.00102	0.27	0.00380	14.23		
9.31	0.00148	0.29	0.00519	19.45		
8.95	0.00316	0.24	0.01304	48.89		
8.95	0.00302	0.23	0.01342	50.29	52.03	2.87
8.95	0.00322	0.22	0.01451	54.40		
8.95	0.00333	0.23	0.01455	54.52		
8.71	0.00187	0.14	0.01329	49.83		
8.71	0.00211	0.15	0.01394	52.27	47.04	4.74
8.71	0.00180	0.16	0.01148	43.02		
8.71	0.00188	0.16	0.01148	43.03		
8.56	0.00147	0.10	0.01453	54.45		
8.56	0.00132	0.12	0.01147	43.00	50.08	6.14
8.56	0.00122	0.10	0.01253	46.96		
8.56	0.00163	0.11	0.01492	55.91		
8.42	0.00252	0.13	0.01893	70.95		
8.42	0.00267	0.13	0.02108	79.03	79.99	6.84
8.42	0.00233	0.10	0.02320	86.98		
8.42	0.00268	0.12	0.02214	82.99		
8.29	0.00407	0.18	0.02272	85.16		
8.29	0.00290	0.18	0.01613	60.47	74.51	11.67
8.29	0.00342	0.18	0.01852	69.42		
8.29	0.00401	0.18	0.02214	83.00		

Table 12: Experimental database to analyse the pH effects in 200-2000μm size-fractioned NADP-IDH activity (2/2)

pH	**NADP-IDH** (μmol NADPH min^{-1}mL^{-1})	**mg protein mL^{-1}**	**NADP-IDH** (μmol NADPH min^{-1}mg protein^{-1})	**%V$_{max}$**	**Average**	**SD**
8.23	0.00599	0.24	0.02506	93.95	93.30	5.10
8.23	0.00507	0.22	0.02346	87.95		
8.23	0.00537	0.22	0.02435	91.29		
8.23	0.00541	0.20	0.02668	100.00		
7.93	0.00293	0.15	0.01957	73.36	66.10	5.13
7.93	0.00263	0.16	0.01639	61.45		
7.93	0.00285	0.17	0.01707	64.00		
7.93	0.00284	0.16	0.01750	65.60		
7.46	0.00264	0.24	0.01077	40.37	41.36	1.54
7.46	0.00261	0.25	0.01064	39.90		
7.46	0.00283	0.25	0.01155	43.30		
7.46	0.00276	0.25	0.01117	41.86		
6.47	0.00056	0.19	0.00290	10.87	9.16	1.27
6.47	0.00043	0.20	0.00213	7.98		
6.47	0.00051	0.20	0.00249	9.35		
6.47	0.00053	0.23	0.00226	8.45		
5.53	0.00004	0.11	0.00032	1.19	3.28	3.78
5.53	0.00007	0.10	0.00071	2.66		
5.53	0.00001	0.11	0.00013	0.49		
5.53	0.00026	0.11	0.00234	8.78		

Table 13: Experimental database to analyse the T effects in 200-2000μm size-fractioned NADP-IDH activity

Sample	T (°C)	NADP-IDH (μmol NADPH min^{-1}mL^{-1})	mg protein mL^{-1}	NADP-IDH (μmol NADPH min^{-1}mg protein^{-1})	%V$_{max}$	Average	SD
200-2000μm	8.1	0.000341	0.25	0.001357	7.65	8.23	0.52
	8.1	0.000375	0.25	0.001489	8.39		
	8.1	0.000386	0.25	0.001533	8.64		
	12.5	0.000697	0.25	0.002772	15.63	14.39	1.14
	12.5	0.000631	0.25	0.002508	14.14		
	12.5	0.000598	0.25	0.002376	13.39		
	16.3	0.001550	0.25	0.006160	34.73	33.65	2.19
	16.3	0.001389	0.25	0.005522	31.13		
	16.3	0.001566	0.25	0.006226	35.10		
	20.4	0.002330	0.25	0.009262	52.21	54.57	2.49
	20.4	0.002424	0.25	0.009636	54.32		
	20.4	0.002552	0.25	0.010142	57.17		
	24.9	0.003583	0.25	0.014241	80.28	77.47	2.46
	24.9	0.003411	0.25	0.013559	76.44		
	24.9	0.003378	0.25	0.013427	75.69		
	29.3	0.004463	0.25	0.017739	100.00	96.32	4.24
	29.3	0.004341	0.25	0.017255	97.27		
	29.3	0.004092	0.25	0.016265	91.69		
	37.2	0.001197	0.25	0.004759	26.83	32.04	4.54
	37.2	0.001568	0.25	0.006233	35.14		
	37.2	0.001524	0.25	0.006057	34.15		
	46.2	0.000411	0.25	0.001635	9.22	5.00	3.73
	46.2	0.000096	0.25	0.000381	2.15		
	46.2	0.000162	0.25	0.000645	3.64		
	54.6	-0.000090	0.25	-0.000359	-2.03	-2.27	3.73
	54.6	0.000059	0.25	0.000235	1.32		
	54.6	-0.000273	0.25	-0.001085	-6.12		

Table 14: Experimental database to analyse the T effects in porcine heart NADP-IDH activity

Sample	T (ºC)	NADP-IDH (μmol NADPH min^{-1}mL^{-1})	mg protein mL^{-1}	NADP-IDH (μmol NADPH min^{-1}mg protein^{-1})	%V$_{max}$	Average	SD
Porcine heart	**8**	0.004286	0.20	0.021260	2.63		
	8	0.004541	0.20	0.022523	2.79	2.76	0.12
	8	0.004662	0.20	0.023127	2.86		
	12.6	0.008651	0.20	0.042913	5.31		
	12.6	0.008939	0.20	0.044341	5.48	5.44	0.11
	12.6	0.008989	0.20	0.044588	5.52		
	16.5	0.015371	0.20	0.076244	9.43		
	16.5	0.015288	0.20	0.075832	9.38	9.41	0.04
	16.5						
	19.3	0.021240	0.20	0.105356	13.03		
	19.3	0.022070	0.20	0.109475	13.54	13.42	0.34
	19.3	0.022297	0.20	0.110600	13.68		
	20.9	0.027094	0.20	0.134395	16.62		
	20.9	0.026839	0.20	0.133132	16.47	16.52	0.09
	20.9	0.026851	0.20	0.133187	16.47		
	25.2	0.052384	0.20	0.259840	32.14		
	25.2	0.050723	0.20	0.251603	31.12	31.19	0.93
	25.2	0.049373	0.20	0.244904	30.29		
	29.3	0.079970	0.20	0.396679	49.07		
	29.3	0.077358	0.20	0.383720	47.46	48.44	0.86
	29.3	0.079528	0.20	0.394483	48.80		
	37.8	0.162782	0.20	0.807452	99.88		
	37.8	0.161742	0.20	0.802290	99.24	99.71	0.41
	37.8	0.162982	0.20	0.808440	100.00		
	46.3	0.114642	0.20	0.568661	70.34		
	46.3	0.120399	0.20	0.597215	73.87	72.02	1.77
	46.3	0.117077	0.20	0.580742	71.83		
	55	0.002081	0.20	0.010323	1.28		
	55	0.003808	0.20	0.018889	2.34	1.74	0.54
	55	0.002613	0.20	0.012959	1.60		

Table 15: Experimental database to analyse the extinction coefficient in solution 1: $MgCl_2$ + isocitrate phosphate buffer

Solution	**NADPH** (mmol L^{-1})	A_{340}	**Average** A_{340}	**SD**	**Linear regression**			
					a (slope)	y_0	r^2	***p-value***
	0.04008	0.231						
	0.04008	0.233	0.232	0.001				
	0.04008	0.231						
	0.02004	0.126						
	0.02004	0.180	0.144	0.031				
	0.02004	0.126						
	0.01002	0.078						
	0.01002	0.070	0.074	0.004				
	0.01002	0.075						
	0.00501	0.053						
	0.00501	0.063	0.057	0.005				
	0.00501	0.054						
	0.00250	0.028						
	0.00250	0.032	0.029	0.003				
	0.00250	0.028						
	0.00125	0.024						
1	0.00125	0.022	0.025	0.003	5.420	0.022	0.9896	<0.0001
	0.00125	0.028						
	0.00063	0.025						
	0.00063	0.023	0.023	0.002				
	0.00063	0.021						
	0.00031	0.029						
	0.00031	0.038	0.033	0.005				
	0.00031	0.031						
	0.00016	0.019						
	0.00016	0.017	0.018	0.001				
	0.00016	0.017						
	0.00008	0.020						
	0.00008	0.018	0.019	0.001				
	0.00008	0.019						
	0.00000	0.022						
	0.00000	0.015	0.019	0.004				
	0.00000	0.022						

Table 16: Experimental database to analyse the extinction coefficient in solution 2: $MgCl_2$ phosphate buffer

Solution	**NADPH** (mmol L^{-1})	A_{340}	**Average** A_{340}	**SD**	**Linear regression**			
					a (slope)	y_0	r^2	***p-value***
	0.04008	0.243						
	0.04008	0.249	0.239	0.012				
	0.04008	0.226						
	0.02004	0.127						
	0.02004	0.118	0.124	0.006				
	0.02004	0.128						
	0.01002	0.075						
	0.01002	0.065	0.070	0.005				
	0.01002	0.072						
	0.00501	0.049						
	0.00501	0.071	0.057	0.013				
	0.00501	0.049						
	0.00250	0.038						
	0.00250	0.032	0.034	0.003				
	0.00250	0.033						
	0.00125	0.026						
2	0.00125	0.020	0.030	0.013	5.348	0.022	0.9916	<0.0001
	0.00125	0.045						
	0.00063							
	0.00063	0.014	0.022	0.011				
	0.00063	0.029						
	0.00031	0.022						
	0.00031	0.024	0.038	0.025				
	0.00031	0.067						
	0.00016	0.016						
	0.00016	0.021	0.018	0.003				
	0.00016	0.018						
	0.00008	0.019						
	0.00008	0.019	0.019	0.000				
	0.00008	0.019						
	0.00000	0.025						
	0.00000	0.015	0.020	0.005				
	0.00000	0.019						

Table 17: Experimental database to analyse the extinction coefficient in solution 3: phosphate buffer

Solution	NADPH (mmol L^{-1})	A_{340}	Average A_{340}	SD	Linear regression a (slope)	y_0	r^2	*p-value*
	0.04008	0.229						
	0.04008	0.235	0.232	0.003				
	0.04008	0.231						
	0.02004	0.130						
	0.02004	0.118	0.127	0.008				
	0.02004	0.133						
	0.01002	0.072						
	0.01002	0.068	0.071	0.003				
	0.01002	0.073						
	0.00501	0.051						
	0.00501	0.050	0.052	0.002				
	0.00501	0.054						
	0.00250	0.061						
	0.00250	0.037	0.047	0.012				
	0.00250	0.043						
	0.00125	0.029						
3	0.00125	0.049	0.046	0.017	5.211	0.023	0.9861	<0.0001
	0.00125	0.062						
	0.00063	0.025						
	0.00063	0.019	0.024	0.005				
	0.00063	0.029						
	0.00031	0.025						
	0.00031	0.021	0.023	0.002				
	0.00031	0.022						
	0.00016	0.010						
	0.00016	0.015	0.014	0.003				
	0.00016	0.016						
	0.00008	0.019						
	0.00008	0.014	0.018	0.004				
	0.00008	0.021						
	0.00000	0.018						
	0.00000	0.012	0.018	0.005				
	0.00000	0.023						

Table 18: Experimental database to analyse the precision of the NADP-IDH assay (pH 8.2, T 37.5°C)

Experiment	UsIDH (μmol NADPH $min^{-1}mL^{-1}$)	UmIDH (μmol NADPH $min^{-1}mL^{-1}$)	Average	SD	Linear regression a (slope)	y_0	r^2	*p-value*
pH 8.2	0.2434	0.1135	0.1155	0.0020	0.482	0.003	0.9882	0.0005
	0.2434	0.1144						
	0.2434	0.1138						
	0.2434	0.1128						
	0.2434	0.1147						
	0.2434	0.1149						
	0.2434	0.1173						
	0.2434	0.1167						
	0.2434	0.1186						
	0.2434	0.1180						
	0.1217	0.0684	0.0693	0.0017				
	0.1217	0.0710						
	0.1217	0.0689						
	0.1217	0.0697						
	0.1217	0.0701						
	0.1217	0.0672						
	0.1217	0.0664						
	0.1217	0.0695						
	0.1217	0.0715						
	0.1217	0.0706						
	0.0243	0.0177	0.0173	0.0006				
	0.0243	0.0176						
	0.0243	0.0177						
	0.0243	0.0181						
	0.0243	0.0178						
	0.0243	0.0175						
	0.0243	0.0172						
	0.0243	0.0163						
	0.0243	0.0170						
	0.0243	0.0167						
	0.0041	0.0018	0.0022	0.0006				
	0.0041	0.0017						
	0.0041	0.0022						
	0.0041	0.0029						
	0.0041	0.0032						
	0.0041	0.0016						
	0.0041	0.0015						
	0.0041	0.0028						
	0.0041	0.0020						
	0.0041	0.0021						
	0.0004	-0.0005	-0.0019	0.0020				
	0.0004	-0.0003						
	0.0004	-0.0011						
	0.0004	0.0006						
	0.0004	0.0002						
	0.0004	-0.0051						
	0.0004	-0.0022						
	0.0004	-0.0042						
	0.0004	-0.0022						
	0.0004	-0.0039						

Table 19: Experimental database to analyse the precision of the NADP-IDH assay(pH 7.4, T 37.5°C)

Experiment	**UsIDH** (μmol NADPH min^{-1}mL^{-1})	**UmIDH** (μmol NADPH min^{-1}mL^{-1})	**Average**	**SD**	**Linear regression**			
					a (slope)	**y_0**	**r^2**	***p-value***
pH 7.4	0.2434	0.0879	0.0926	0.0048	0.393	0.004	0.9606	0.0034
	0.2434	0.0852						
	0.2434	0.0870						
	0.2434	0.0910						
	0.2434	0.0924						
	0.2434	0.0965						
	0.2434	0.0944						
	0.2434	0.0938						
	0.2434	0.0985						
	0.2434	0.0990						
	0.1217	0.0632	0.0645	0.0018				
	0.1217	0.0625						
	0.1217	0.0637						
	0.1217	0.0630						
	0.1217	0.0633						
	0.1217	0.0663						
	0.1217	0.0631						
	0.1217	0.0666						
	0.1217	0.0670						
	0.1217	0.0662						
	0.0243	0.0170	0.0168	0.0003				
	0.0243	0.0170						
	0.0243	0.0172						
	0.0243	0.0167						
	0.0243	0.0163						
	0.0243	0.0168						
	0.0243	0.0166						
	0.0243	0.0171						
	0.0243	0.0170						
	0.0243	0.0167						
	0.0041	0.0011	0.0012	0.0006				
	0.0041	0.0010						
	0.0041	0.0002						
	0.0041	0.0009						
	0.0041	0.0015						
	0.0041	0.0016						
	0.0041	0.0009						
	0.0041	0.0007						
	0.0041	0.0016						
	0.0041	0.0023						
	0.0004	-0.0017	-0.0018	0.0007				
	0.0004	-0.0027						
	0.0004	-0.0019						
	0.0004	-0.0014						
	0.0004	-0.0016						
	0.0004	-0.0010						
	0.0004	-0.0012						
	0.0004	-0.0033						
	0.0004	-0.0019						
	0.0004	-0.0011						

Table 20: Experimental database to analyse the limit of detection of the NADP-IDH assay

Samples	Biomass (mg proteins)	NADP-IDH (μmol NADPH $min^{-1}mL^{-1}$)	Average	SD	Linear regression a (slope)	y_0	r^2	*p-value*
200-2000μm	0.684	0.00891						
	0.684	0.00840	0.00847	0.00040				
	0.684	0.00811						
	0.342	0.00443						
	0.342	0.00345	0.00435	0.00086				
	0.342	0.00516						
	0.171	0.00259						
	0.171	0.00262	0.00257	0.00007				
	0.171	0.00249						
	0.085	0.00102						
	0.085	0.00148	0.00116	0.00028				
	0.085	0.00099						
	0.043	0.00082						
	0.043	0.00090	0.00081	0.00010	0.012	0.000	0.9971	<0.0001
	0.043	0.00070						
	0.021	0.00044						
	0.021	0.00016	0.00035	0.00016				
	0.021	0.00044						
	0.011	0.00012						
	0.011	0.00014	0.00012	0.00001				
	0.011	0.00012						
	0.005	0.00012						
	0.005	0.00003	0.00017	0.00017				
	0.005	0.00035						
	0.003	0.00001						
	0.003	0.00002	0.00001	0.00001				
	0.003	0.00002						
0.7-50μm	0.083	0.00136						
	0.083	0.00138	0.00138	0.00002				
	0.083	0.00141						
	0.066	0.00129						
	0.066	0.00117	0.00123	0.00006				
	0.066	0.00123						
	0.050	0.00079						
	0.050	0.00081	0.00077	0.00005				
	0.050	0.00073						
	0.033	0.00054						
	0.033	0.00050	0.00055	0.00006	0.017	0.000	0.9875	<0.0001
	0.033	0.00062						
	0.017	0.00034						
	0.017	0.00024	0.00030	0.00005				
	0.017	0.00030						
	0.008	0.00019						
	0.008	0.00019	0.00020	0.00002				
	0.008	0.00022						
	0.004	0.00010						
	0.004	0.00006	0.00006	0.00004				
	0.004	0.00003						

Table 21: Experimental database to analyse the dilution effects on NADP-IDH activity

Samples	Sample concentration (%)	% Vmax	Average	SD	Linear regression a (slope)	y_0	r^2	*p-value*
200-2000μm	100.00	100.00						
	100.00	94.28	95.11	4.53				
	100.00	91.05						
	50.00	49.78						
	50.00	38.72	48.83	9.67				
	50.00	57.99						
	25.00	29.09						
	25.00	29.46	28.82	0.81				
	25.00	27.91						
	12.50	11.44						
	12.50	16.66	13.07	3.11				
	12.50	11.12						
	6.25	9.20						
	6.25	10.07	9.05	1.09	0.946	1.484	0.9971	<0.0001
	6.25	7.89						
	3.13	4.91						
	3.13	1.80	3.87	1.79				
	3.13	4.91						
	1.56	1.31						
	1.56	1.55	1.39	0.14				
	1.56	1.31						
	0.78	1.37						
	0.78	0.31	1.86	1.85				
	0.78	3.92						
	0.39	0.06						
	0.39	0.19	0.17	0.09				
	0.39	0.25						
0.7-50μm	100.00	96.85						
	100.00	98.03	98.29	1.59				
	100.00	100.00						
	80.00	91.73						
	80.00	83.07	87.53	4.34				
	80.00	87.80						
	60.00	55.91						
	60.00	57.87	55.12	3.22				
	60.00	51.57						
	40.00	38.58						
	40.00	35.43	39.37	4.38	0.994	0.940	0.9875	<0.0001
	40.00	44.09						
	20.00	24.41						
	20.00	17.32	21.00	3.55				
	20.00	21.26						
	10.00	13.39						
	10.00	13.39	14.17	1.36				
	10.00	15.75						
	5.00	7.09						
	5.00	3.94	4.33	2.58				
	5.00	1.97						

Table 22: Experimental database to analyse the stability of the enzyme preparation in *L. lingvra* samples

Time (min)	**NADP-IDH** (μmol NADPH min^{-1} mL of homogenate^{-1})	**NADP-IDH** (%Vmax)	**Average** (%Vmax)	**SD**	**Linear regression**			
					a (slope)	**y_0**	**r^2**	***p*-value**
0	0.0085	100.00						
0	0.0084	97.86	97.76	2.30				
0	0.0082	95.40						
85	0.0068	79.80						
85	0.0069	80.90	80.84	1.01				
85	0.0070	81.81						
146	0.0063	73.13						
146	0.0061	71.77	74.32	3.30				
146	0.0067	78.05						
228	0.0050	59.02						
228	0.0056	65.88	63.53	3.91				
228	0.0056	65.69						
312	0.0048	55.98			-0.109	92.357	0.9771	<0.0001
312	0.0051	59.99	58.07	2.01				
312	0.0050	58.24						
376	0.0043	50.22						
376	0.0044	51.12	51.17	0.97				
376	0.0045	52.16						
450	0.0039	45.49						
450	0.0040	47.11	46.20	0.83				
450	0.0039	46.01						
511	0.0028	32.28						
511	0.0034	40.18	37.14	4.25				
511	0.0033	38.95						